bioRxiv preprint doi: https://doi.org/10.1101/029892; this version posted January 25, 2016. The copyright holder for this preprint (which was not certified by peer review) is the author/funder, who has granted bioRxiv a license to display the preprint in perpetuity. It is made available under aCC-BY 4.0 International license.

Expression of segment polarity genes in brachiopods supports a nonsegmental ancestral role of *engrailed* for bilaterians

Bruno C. Vellutini[1] and Andreas Hejnol[2*]

[1,2]Sars International Centre for Marine Molecular Biology, University of Bergen, Thormøhlensgate 55, 5008 Bergen, Norway.

[1]Email: bruno.vellutini@uib.no

[2]Email: andreas.hejnol@uib.no

[*]Corresponding author.

Keywords: Brachiopoda, larvae, segmentation, boundary, *engrailed*, *wnt1*, *hedgehog*, *pax6*, *pax2/5/8*

Abstract

Brachiopods are benthic marine invertebrates that live enclosed in a bivalved shell. Despite having a reduced and unsegmented trunk in the adult stage, brachiopod larvae show putative segmented structures such as transverse ectodermal boundaries and iterated coelomic sacs. Several molecular mechanisms of segmentation have been described in animals considered to be segmented (i.e., the distantly related annelids, arthropods and vertebrates), but far less is known about the role of these "segmentation genes" in other organisms. Here we investigate the expression of the arthropod segment polarity genes *engrailed*, *wnt1* and *hedgehog* in the development of brachiopods—a group more closely related to the segmented annelids. Expression of *engrailed* correlates with the development of an anterior nonsegmental ectodermal boundary in the embryos of *Terebratalia transversa* and *Novocrania anomala*. Surprisingly, *wnt1* is expressed as a stripe adjacent to *engrailed* in *T. transversa* in the same manner as in the parasegment boundaries of insects. Expression of *hedgehog*, however, is restricted to the endoderm and is not compatible with a segment polarity role. In addition, the putative *engrailed* regulators *pax6* and *pax2/5/8* encircle the whole embryo and demarcate this anterior ectodermal boundary before *engrailed*. We conclude brachiopod larvae might have a common anterior patterning involving the expression of *pax6*, *pax2/5/8* and *engrailed*. Despite key differences to other segment boundaries (e.g., *hedgehog* expression), we show the characteristic adjacent stripes of *engrailed* and *wnt1* can occur in a nonsegmental ectodermal boundary. A comparison among bilaterians suggests the ancestral expression of *engrailed* during early development was nonsegmental and conceivably related to the embryonic head/trunk boundary. Our data implies that *engrailed* was independently recruited to the segment boundaries of annelids and arthropods and to other different developmental boundaries during evolution.

bioRxiv preprint doi: https://doi.org/10.1101/029892; this version posted January 25, 2016. The copyright holder for this preprint (which was not certified by peer review) is the author/funder, who has granted bioRxiv a license to display the preprint in perpetuity. It is made available under aCC-BY 4.0 International license.

Background

Animals with bilateral symmetry show a great diversity of serially repeated structures along the body. Neural ganglia, excretory organs, coeloms, and a variety of other tissues can be individually arranged in a serial manner or combined into repetitive body segments. The repetition of parts with anteroposterior polarity along the body axis is a defining characteristic of animal segmentation (Budd 2001; Hannibal & Patel 2013; Minelli & Fusco 2004). Groups like annelids (*e.g.*, earthworms), arthropods (*e.g.*, insects) and vertebrates (*e.g.*, humans) segment their embryonic tissues from anterior to posterior and have a major part of their adult body organized into repeated units. Therefore, these groups have been the main focus of studies on the evolution of segmentation.

Comparative developmental data revealed a number of similarities in the molecular mechanisms of segmentation between arthropods and vertebrates (Damen 2007; Davis & Patel 1999; Kimmel 1996; Patel 2003; Seaver 2003; Tautz 2004), that were taken as evidence to support the homology of bilaterian segmentation (De Robertis 1997, 2008; Dray *et al.* 2010; Kimmel 1996). However, annelids, arthropods and vertebrates belong to distinct branches of bilaterally symmetrical animals, spiralians, ecdysozoans and deuterostomes, respectively (Figure 1A), suggesting alternatively that these molecular similarities are evolutionary convergences (Abouheif *et al.* 1997; Chipman 2010; Minelli & Fusco 2004). The sole comparison between such distantly related groups can be misleading for tracing the evolution of a character (*e.g.*, trunk segmentation) because the ancestral conditions of related taxa are unknown. Since developmental mechanisms can be coopted to nonhomologous structures (Shubin *et al.* 2009), knowing the phylogenetic context of a character is essential to distinguish homology from convergence. Furthermore, segmentation is not restricted to annelids, arthropods and vertebrates. It also occurs in other bilaterians usually considered as pseudosegmented or unsegmented (Budd 2001; Minelli & Fusco 2004; Scholtz 2002). To fully understand the conservation of gene networks in the evolution of segmentation, it is important to uncover the expression and role of genes guiding body segmentation of annelids, arthropods and vertebrates in the development of other animals, as well as to understand their relationship to other serially repeated structures.

A crucial mechanism of segmentation is the ability to establish tissue boundaries during animal development (Dahmann *et al.* 2011). One of the best studied developmental boundaries are the parasegmental boundaries of the fruit fly *Drosophila melanogaster*. Fly segmentation occurs by the simultaneous division of the trunk into fourteen parasegments, developmental regions that lie out of register with the larval segments (Martinez-Arias & Lawrence 1985). At the molecular level, the parasegment boundary is established by the abutting domains of *engrailed* (*en*) and *wingless* (*wnt1*) (Ingham *et al.* 1988) and maintained by a positive feedback loop mediated by *hedgehog* (*hh*) (Ingham & Martinez Arias 1992). Therefore, *en*, *wnt1* and *hh* are commonly referred to as segment polarity genes (Ingham 1991; Martinez Arias *et al.* 1988; Tabata & Kornberg 1994), and their expression and function seems to be conserved among the body segments of other arthropods (Damen 2007; Hughes & Kaufman 2002; Mellenthin *et al.* 2006; Nagy 1994). Similarity in the expression of segment polarity genes was used to claim homology of arthropod and annelid segmentation (Dray *et al.* 2010; Prud'homme *et al.* 2003), however their role in annelids is unclear. In *Platynereis dumerilii*, the expression of *en*, *wnt1* and *hh* supports a role in estab-

bioRxiv preprint doi: https://doi.org/10.1101/029892; this version posted January 25, 2016. The copyright holder for this preprint (which was not certified by peer review) is the author/funder, who has granted bioRxiv a license to display the preprint in perpetuity. It is made available under aCC-BY 4.0 International license.

lishing the segment boundaries of this animal (Prud'homme *et al.* 2003), whereas other annelid species do not show a spatial correlation of these genes with the segmental boundaries (Seaver & Kaneshige 2006). Thus, it is of utmost importance to investigate the segment polarity genes in groups closely related to annelids and arthropods to infer their ancestral developmental functions, and verify if similar expression patterns are deployed in different morphological structures.

Brachiopods are bivalved marine invertebrates closely related to annelids (Laumer *et al.* 2015) (Figure 1A). Even though adult brachiopods do not have a segmented trunk, the larval stages of different groups show putative repeated structures in different parts of their body. Externally, brachiopod larvae exhibit two to four lobes along the anteroposterior axis divided by transverse ectodermal boundaries. In the past, brachiopod larval lobes were homologized to annelid segments (Balfour 1880), but the observation that the ectodermal boundaries do not involve the underlying mesoderm weakened this hypothesis (Conklin 1902). Mesoderm morphology, however, is variable between brachiopod species, and can be unsegmented or indeed partitioned into two or four pairs of coelomic sacs (Hyman 1959; Nielsen 1991). The existence of brachiopod larvae with serially arranged mesodermal coelomic sacs has revived the idea that brachiopods had a segmented ancestor (Balavoine & Adoutte 2003; Temereva & Malakhov 2011). Therefore, the putative segmentation of brachiopod larvae is key to comprehend the evolution of segmentation mechanisms because it provides a closer phylogenetic comparison for the role of the segment polarity genes in the annelids.

To investigate the developmental and molecular background of the repeated structures of brachiopod larvae, we studied the trilobed larva with unsegmented mesoderm of *Terebratalia transversa* (John A. Long and Stephen A. Stricker 1991) (Figure 1B), and the bilobed larva with four pairs of coelomic sacs of *Novocrania anomala* (Freeman 2000; Nielsen 1991) (Figure 1B). In these two species of brachiopods, we analyzed the expression of the segment polarity genes *en*, *wnt1*, and the core components of the Hedgehog signaling pathway to test whether their expression correlate with the development of the ectodermal and mesodermal boundaries of *T. transversa* and *N. anomala* larvae. Furthermore, we examined upstream control genes of *en* and discovered unexpected similarities in the molecular profile of a brachiopod larval lobe boundary and a vertebrate brain boundary.

Results

Ectodermal and mesodermal boundaries of larval brachiopods

In *T. transversa*, gastrulation occurs by invagination and results in a radially symmetric gastrula (Figure 2A). After anteroposterior axis elongation (Figure 2B), the embryos adopt the definitive bilateral morphology (Figure 2C). At this stage, a transverse ectodermal furrow (indentation of the epidermis) appears around the circumference of the bilateral gastrula extending from the blastopore lips above the midline to most of the dorsal side (Figure 2C; Figure 3A). Epidermal cells abutting the posterior border of the furrow are more elongated along the furrow outline when compared to the isodiametric shape of anterior and posterior cells (Figure 3B). The ectodermal furrow at the bilateral gastrula is the first morphological manifestation of the boundary between the apical and mantle lobes in *T. transversa* (apical/mantle boundary). At subsequent developmental stages, this furrow deepens and clearly divides the apical lobe from the remainder of the embryo (Figure 2D; Figure 3C,D). *T. transversa* exhibits a third lobe at the posterior end, the pedicle lobe (Figure 2E). The boundary

bioRxiv preprint doi: https://doi.org/10.1101/029892; this version posted January 25, 2016. The copyright holder for this preprint (which was not certified by peer review) is the author/funder, who has granted bioRxiv a license to display the preprint in perpetuity. It is made available under aCC-BY 4.0 International license.

between the mantle and pedicle lobes (mantle/pedicle boundary) is identified by the narrowing of the posterior portion of the embryo (Figure 2D) and by the subsequent outgrowth of the mantle lobe (Figure 2E). The morphology of the mantle/pedicle boundary differs from the apical/mantle boundary because it is demarcated by an ectodermal fold, rather than an indentation furrow. Thus, despite the superficial impression of ectodermal segmentation in the brachiopod trilobed larva, these boundaries are not repeated, but unique structures of the larval body. *N. anomala* also gastrulates by invagination and elongates along the anteroposterior axis (Figure 2F–H). Its apical and mantle lobes are demarcated by an ectodermal furrow, as seen in *T. transversa* (Figure 2H–J; Figure 3E–G), but the larva of *N. anomala* does not form a pedicle lobe (Figure 2J; Figure 3H). Thus, the morphology of the apical/mantle boundary is conserved between both species suggesting it is an ancestral feature of larval brachiopods.

In the trilobed larva of *T. transversa*, the mesoderm is unsegmented and has a distinct anterior portion in the apical lobe, an umbrella-like mesoderm in the mantle lobe connected to the chaetae sacs and, finally, an arrowhead-shaped pedicle portion (Figure 3I–L). Unlike *T. transversa*, the mesoderm of *N. anomala* has lateral constrictions individualizing each of the four pairs of coelomic sacs (Figure 3M) while remaining interconnected more medially in the ventral side (Figure 3N). From the second, third and fourth coelomic pouches we observe dorsal projections of the mesoderm associated to the three pairs of chaetae sac primordia (Figure 3N,O). In the bilobed larva, this arrangement is compacted and an extensive musculature develops; coelomic spaces are reduced (Figure 3O,P). Thus, the segmented appearance of *N. anomala* mesoderm is related to its partitioning into coelomic sacs with tight association to the seriated chaetae sacs on the dorsal side.

Expression of the segment polarity genes *hh*, *en* and *wnt1*

In order to understand the developmental and phylogenetic relationship of the ectodermal and mesodermal boundaries of brachiopods with those of the body segments of arthropods and annelids, we analyzed the expression of the segment polarity genes *en*, *wnt1* and *hh* during the embryonic development of *T. transversa* and *N. anomala*. Expression of *hh* localizes to the blastoporal lip and invaginating endomesoderm during the early gastrulation of *T. transversa* (Figure 4A1); in later stages it is restricted to the endoderm (Figure 4A2–A4). In *N. anomala*, we detected a transverse ventral stripe of *hh* near the animal pole and (additionally) along the blastoporal lip at the asymmetric gastrula (Figure 4B1). Endodermal transcripts only became visible at the bilateral gastrula (Figure 4B2). The anterior ventral stripe of *hh* expression in *N. anomala* is reduced and disappears in the bilobed larva while endodermal transcripts continue to be expressed (Figure 4B3–B4). Therefore, the expression of *hh* orthologs in *T. transversa* and *N. anomala* does not correlate spatially or temporally with the development of the ectodermal larval lobe boundaries.

Since the Hedgehog ligand can signal across embryonic layers, we further analyzed the expression of the Hedgehog receptors *ptc* and *smo* and the transcription factor *gli*. Transcripts are expressed in the mesoderm of *T. transversa* and *N. anomala*, as well as in the ectodermal apical and mantle territories (Additional file 1: Figure S1). Altogether, the expression of *hh* and downstream pathway components does not support a connection of this signaling pathway with the ectodermal boundaries of both brachiopod species.

bioRxiv preprint doi: https://doi.org/10.1101/029892; this version posted January 25, 2016. The copyright holder for this preprint (which was not certified by peer review) is the author/funder, who has granted bioRxiv a license to display the preprint in perpetuity. It is made available under aCC-BY 4.0 International license.

Transcripts of *T. transversa en* were first detected in the radial gastrula as an almost complete ring in the midregion of the embryo (Additional file 2: Figure S2A). Expression fades at the anterior end and subsequently clears from the posterior end leaving a pair of lateral domains of *en* in the late radial gastrula (Additional file 2: Figure S2A–H) and asymmetric gastrula (Figure 4C1). These domains extend ventrally and dorsally without reaching the blastopore on the ventral side (Figure 4C2). Transcripts of *en* border the apical/mantle furrow in the subsequent stage (Figure 4C3) and fade in the developed larvae (Figure 4C4). In *N. anomala* a single dorsal ectodermal stripe of *en* expression occurs in the radial gastrula (Additional file 2: Figure S2I) and a second stripe emerges at the posterior end of the asymmetric gastrula (Figure 4D1; Additional file 2: Figure S2J). Similar to *T. transversa*, *en* stripes extend ventrally without reaching the embryo midline (Figure 4D1–D3) and fade in the developed larva (Figure D4). Therefore, expression of *en* is consistent between the two species, with the apical/mantle furrow forming immediately anterior to a pair of *en* stripes.

In addition to the striped domains demarcating the apical/mantle furrow, we identified two more posterior *en* territories on the ventral and dorsal regions of larval brachiopods, localized in the anterior-most region of the pedicle lobe. A pair of *en* ectodermal bands initiate on the ventral side of *T. transversa* associated with the blastopore (Figure 4C2). On the opposite side, at the center of the dorsal surface, we detected a triangular-shaped domain of *en* expression (Figure 4C2; Additional file 2: Figure S2N–O). Expression is still present in the trilobed larva of *T. transversa* (Figure 4C4). A reciprocal dorsal domain also occurs in *N. anomala* bilateral gastrula (Additional file 2: Figure S2K) and localizes to the shell rudiment in the bilobed larva (Additional file 2: Figure S2L,M).

Until the asymmetric gastrula, transcripts of *en* in *T. transversa* are restricted to the ectoderm (Figure 4C1,G). Mesodermal expression of *en* only initiates at the bilateral gastrula (Figure 4C2,H). A thin line of *en*-expressing cells suggests contiguous expression between ectoderm and mesoderm (Figure 4C2,J). Transcripts of *en* form a pair of mesodermal bands posterior to the ventral projections of the mantle mesoderm (Figure 4I,K,L). In the asymmetric gastrula of *N. anomala* we only detected weak *en* expression in the mesoderm (Figure 4M). Expression of *en* becomes stronger localizing directly inner to the lateral ectodermal domains (Figure 4N). This region corresponds to the posterior portion of the second pair of coelomic pouches. Transcripts of *en* are also detected in the posterior region of the third pair of coeloms in the bilobed larva, but not in the first or fourth coelomic sacs (Figure 4O–R). Expression in the second coelomic sac localizes to the medial portion of the mesoderm (Figure 4P,Qi) while the expression in the third coelomic sac is more lateral and ventral (Figure 4P inset, Qii). Overall, the mesodermal expression of *en* occurs in contiguity with the preceding ectodermal domains in both species.

Expression of *wnt1* in the asymmetric gastrula of *T. transversa* is associated with the posterior portion of the blastopore (Figure 4E1) and shows no spatial correlation to the lateral *en* domains (Figure 5A). At the bilateral gastrula, a transverse pair of stripes of *wnt1* expression appears in the apical lobe of *T. transversa* bordering the apical/mantle furrow anteriorly (Figure 4E2). The expression abuts *en* at the apical/mantle furrow without overlap (Figure 5B). In the pedicle lobe, *en* partially overlaps with the posterior domain of *wnt1* (Figure 4E2; Figure 5B). Transcripts of *wnt1* are not present on the dorsal surface at this stage (Figure 4E2; Additional file 2: Figure S2P). As the apical/mantle furrow deepens in the bilobed larva, *wnt1* and *en* transcripts resolve into well-defined non-overlapping stripes in *T. transversa* (Figure

bioRxiv preprint doi: https://doi.org/10.1101/029892; this version posted January 25, 2016. The copyright holder for this preprint (which was not certified by peer review) is the author/funder, who has granted bioRxiv a license to display the preprint in perpetuity. It is made available under aCC-BY 4.0 International license.

5C). Stripes demarcate precisely the morphological furrow at the apical/mantle boundary of *T. transversa* with *wnt1* positioned anterior and *en* positioned posterior to the furrow (Figure 5C). At the bilobed larva, *wnt1* expression initiates on the dorsal side (Figure 4E3; Additional file 2: Figure S2Q) and we observe tight coexpression of *en* and *wnt1* at the dorsal and ventral domains (Figure 5C). Expression of *wnt1* in the apical lobe fades in the trilobed larva (Figure 4E4) while an additional stripe of *wnt1* encircles a subdivision of the pedicle lobe (Figure 4E4).

Differently, *N. anomala* does not have *wnt1* domains in the apical lobe and transcripts are exclusively localized at the posterior end associated with the blastopore (Figure 4F1–F4). While *en* and *wnt1* are coexpressed on the ventral and dorsal territories of *T. transversa*, we did not detect any coexpression sites for these genes in *N. anomala*. Thus, the expression of *wnt1* at the apical/mantle furrow is not consistent between brachiopods, and only *T. transversa* has *wnt1* stripes demarcating the morphology of the furrow.

Expression of the putative *engrailed* regulators *pax6*, *pax2/5/8* and *fgf8/17/18*

The only gene consistently related to the apical/mantle furrow in both brachiopod larvae is *en*. Early expression of *en*, however, does not encircle the circumference of the embryo (Figure 4C1) suggesting that there must be factors upstream positioning the apical/mantle boundary. Regulators of *en* are mostly known from the body segmentation of fruit flies and the brain development of vertebrates. In *D. melanogaster*, activity of *even-skipped* (*eve* or *evx*) position *en* stripes by repressing *sloppy paired* (*slp* or *foxg*), which in turn limits *en* expression anterior to the parasegment boundary (Cadigan *et al.* 1994; Fujioka *et al.* 2002). However, expression of *eve* and *slp* does not correlate to the *en* domains at the apical/mantle boundary of *T. transversa*; *eve* is expressed at the posterior end of the pedicle lobe, while *slp* is expressed at the anterior portion of the apical lobe (Santagata *et al.* 2012). In the vertebrate brain, *en* and *wnt1* play a crucial role in the establishment of the mid/hindbrain boundary (Rhinn & Brand 2001). In the midbrain, *pax2* regulates the expression of *en* in a positive feedback loop, while it represses *pax6* (Okafuji *et al.* 1999). Expression of *pax6* in the forebrain downregulates the expression of *en1* and *pax2* in the midbrain, while *en* was shown to directly repress the expression of *pax6* (Araki & Nakamura 1999; Matsunaga *et al.* 2000; Scholpp *et al.* 2003). The regulation between *pax6*, *en* and *pax2/5/8* results in complementary expression patterns that define the boundary between the diencephalon and mesencephalon (Araki & Nakamura 1999; Matsunaga *et al.* 2000) dependent on *fgf8* signaling from the mid/hindbrain boundary (Scholpp *et al.* 2003). Thus, we analyzed the expression of the brachiopod orthologs of *pax6*, *pax2/5/8* and *fgf8/17/18* in relation to the *en* expression and the development of the apical/mantle furrow.

Expression of *pax6* in the larva of *T. transversa* localizes to the apical lobe and is related to eye development (Passamaneck *et al.* 2011). During earlier stages in *T. transversa*, however, we detected *pax6* transcripts in a broad pair of anterior domains (Figure 6A1). The expression of *pax6* occupies the entire anterior half of the radial gastrula and localizes to the apical lobe in subsequent stages (Figure 6A2–A4). Expression of *pax6* in *N. anomala* initiates as an apical ring in the radial gastrula (Figure 6B1) and localizes to the apical lobe during later stages (Figure 6B2–B4). In both species the posterior limit of *pax6* expression borders the apical/mantle furrow.

bioRxiv preprint doi: https://doi.org/10.1101/029892; this version posted January 25, 2016. The copyright holder for this preprint (which was not certified by peer review) is the author/funder, who has granted bioRxiv a license to display the preprint in perpetuity. It is made available under aCC-BY 4.0 International license.

T. transversa pax2/5/8 expression begins as a posterior half-ring in the radial gastrula (Figure 6C1) and shows a narrow overlap with the *pax6* territory at the future apical/mantle furrow (Figure 7A,B). In the asymmetric gastrula *pax2/5/8* transcripts cover the whole extension of the mantle ectoderm except chaetae sac primordia and blastoporal lips (Figure 6C2). The lateral domains of *en* expression are contained within the mantle lobe domain of *pax2/5/8* (Figure 7G). The anterior limit of *pax2/5/8* expression extends across the apical/mantle furrow (Figure 6C3,C4) and overlaps with *pax6* expression at the posteriormost region of the apical lobe (Figure 7C,D). The fact that the *pax2/5/8* domain transpasses the ectodermal furrow was corroborated by the combined expression with *en* (Figure 7H–J). The arrangement between *pax6*, *pax2/5/8* and *en* domains is maintained in the bilobed larva (Figure 7D,J) but dissociates at the onset of mantle outgrowth. Expression of *pax6* becomes restricted dorsally, and *pax2/5/8* expression localizes to the edge of the growing mantle lobe (Figure 7E,F). Similar to *T. transversa*, *N. anomala pax2/5/8* expression occurs in a posterodorsal territory in the mantle lobe (Figure 6D1) limited by the apical lobe (Figure 6D2,D3). Differently than *T. transversa*, we observe mesodermal expression of *pax2/5/8* in *N. anomala*, which correlates with coelom formation (Figure 6D4). Transcripts of *pax2/5/8* are localized to two pairs of domains between the chaetae sacs of *N. anomala* larval mesoderm (Figure 6D4). In summary, *pax6* and *pax2/5/8* are expressed in early complementary domains encircling the whole embryo with a narrow overlap. The posterior limit of *pax6* matches the apical/mantle furrow and abuts the lateral patches of *en* contained within the mantle lobe domain of *pax2/5/8*.

In the vertebrate brain, *fgf8* expression borders the mid/hindbrain boundary with the adjacent expression of *wnt1* (Danielian & McMahon 1996). We detected transcripts of *fgf8/17/18* in an anterior half-ring of *T. transversa* radial gastrula (Figure 6E1). In the asymmetric gastrula, *fgf8/17/18* is expressed in transverse ventral bands reaching the blastopore lips and two pairs of circular spots positioned laterally and dorsally (Figure 6E2). A new domain at the anterior tip and an additional pair of lateral spots are activated in the bilateral gastrula (Figure 6E3). The circular spots of *fgf8/17/18* positive cells correspond to the developing chaetae sacs (Figure 7K,N) and are cleared from *en* and *pax2/5/8* expression (Figure 7I,K). Ventral bands of *fgf8/17/18* do not border the stripes of *en* posterior to the furrow (Figure 7L,M). In the bilobed larva of *T. transversa* the expression in the chaetae sacs becomes interconnected, the ventral domains in the apical lobe faded and a new domain appeared at the posterior tip (Figure 6E4). In *N. anomala*, *fgf8/17/18* is not expressed in the radial gastrula (Figure 6F1). Expression initiates in the asymmetric gastrula with an anterior ventral band and a more posterior domain encircling the vegetal portion near the blastopore (Figure 6F2). The anterior band extends dorsally while the posterior domain forms a band that demarcates the anterior-most region of the mantle lobe (Figure 6F3). Similarly to *T. transversa*, chaetae primordia also express *fgf8/17/18* (Figure 6F3,F4). Thus, the expression of *fgf8/17/18* is mainly associated with the chaetae sacs in both species and does not show clear correlation with ectodermal boundaries.

Over-activation of the Wnt pathway in *T. transversa*

Because Wnt signaling has an essential role in the axial patterning of metazoans (Petersen & Reddien 2009), we investigated if perturbing the canonical Wnt pathway affects the development of larval boundaries in *T. transversa*. Over-activation of the Wnt pathway with 1-azakenpaullone (Kunick *et al.* 2004) at the mid-blastula and radial gastrula stage leads to the posteriorization of the embryonic axis (e.g. expansion of the pedicle lobe) and a correspondent anterior shift in the expression domains of

bioRxiv preprint doi: https://doi.org/10.1101/029892; this version posted January 25, 2016. The copyright holder for this preprint (which was not certified by peer review) is the author/funder, who has granted bioRxiv a license to display the preprint in perpetuity. It is made available under aCC-BY 4.0 International license.

en, *wnt1* and *pax6* in *T. transversa* (Figure 8). Embryos treated at the mid-blastula stage show no morphological or molecular traces of a mantle lobe (Figure 8B,R,S), but form a distinct anterior portion which folds over the over-developed pedicle lobe (Figure 8R). Interestingly, embryos treated at a later stage (radial gastrula) develop bilateral stubs, which we interpret as incipient mantle tissue due to their mid-body position (Figure 8J). Finally, the ectodermal furrow does not form at the expected apical/mantle boundary in embryos treated at the radial gastrula (Figure 8J; Additional file 3: Figure S3). While all treated embryos show an anterior shift in the expression of *en*, *wnt1* and *pax6*, early treatments at the mid-blastula stage entirely abolish the anterior domains of *en* and *wnt1* (Figure 8D,F), but do not suppress the expression of *pax6* (Figure 8H).

Discussion

Segmentation is an unequivocal feature of annelids, arthropods and vertebrates, and widespread to different degrees in other animals with bilateral symmetry, yet we have little idea on how segmentation mechanisms have evolved and how the segmented structures between these lineages are related. One approach to better understand the evolution of segmentation is to expand the taxonomic sampling. Studying common segmentation genes in other animals can help distinguish which molecular pathways are unique to segmentation and reveal additional—and possibly ancestral—roles of these genes. In this sense, brachiopods are well suited because their larval bodies have putative segmented structures divided by ectodermal and mesodermal boundaries. But, do larval brachiopods have any kind of body segmentation?

Larval brachiopods do not have body wall segmentation

The body wall of *T. transversa* larva is divided into three lobes by two transverse ectodermal boundaries. If these lobes were repeated units, we would expect to find similar morphological characters and molecular topologies at these boundaries. Instead, the apical/mantle boundary is demarcated by an indentation furrow while the mantle/pedicle boundary is demarcated by an ectodermal fold. These morphological differences indicate the lobe boundaries of a trilobed brachiopod larva are not repeated, but unique structures of the larval body. In addition, the molecular profiles at the apical/mantle and mantle/pedicle boundaries differ, further supporting the idea that the body wall of brachiopod larvae has no segmentation.

We found a mosaic of similarities and differences in the patterns of gene expression of *T. transversa* and *N. anomala*. By checking the consistency of a particular domain between the two brachiopod species, we determined which expression patterns are likely to reflect the ground pattern of brachiopod development. Therefore, the apical/mantle boundary is characterized by the early overlapping expression of *pax6* and *pax2/5/8* in the apical and mantle lobes, respectively, with the latter containing a pair of lateral *en* domains (Figure 9A). Expression of *en* expands lining the posterior border of the furrow with the abutting domain of *pax6* anteriorly (Figure 9A). Surprisingly, the pedicle lobe domain of *en* in the trilobed larva of *T. transversa* has a reciprocal domain in the bilobed larva of *N. anomala*, even though there is no morphological evidence of a pedicle lobe or mantle/pedicle boundary in the latter. This observation suggests that two pairs of lateral *en* domains is the ancestral condition for brachiopods independent of the trilobed or bilobed larval morphology.

bioRxiv preprint doi: https://doi.org/10.1101/029892; this version posted January 25, 2016. The copyright holder for this preprint (which was not certified by peer review) is the author/funder, who has granted bioRxiv a license to display the preprint in perpetuity. It is made available under aCC-BY 4.0 International license.

Over-activation of the Wnt pathway abolishes *en* and *wnt1* but not *pax6* expression at the apical/mantle boundary

Over-activation of the Wnt pathway caused an expansion of the pedicle lobe and of the domains of gene expression therein, suppressed the formation of the mantle lobe and of the apical/mantle furrow, and shifted other expression domains anteriorly. Because embryos treated at the mid-blastula stage show no morphological or molecular traces of a mantle lobe, we suggest the boundary between the anterior and posterior portions of treated larvae does not correspond to any of the wild type boundaries, but to a unique apical/pedicle boundary defined by an ectodermal fold. However, embryos treated at later stages (radial gastrula) show bilateral stubs of mantle tissue, suggesting the specification of the mantle lobe of *T. transversa* might initiate between mid-blastula and radial gastrula stage. The period between mid-blastula and early gastrulation can also play a role in the positioning of the anterior domains of *en* and *wnt1* —but not in the establishment of *pax6* expression. Disturbance of *en* and *wnt1* expression in the mid-blastula treatments suggests these anterior domains are not yet established in the embryo, and their positioning is affected by the over-activation of the Wnt pathway. Differently, the consistent expression of *pax6* between mid-blastula and radial gastrula treatments indicates the anterior domain of *pax6* was not affected by the azakenpaullone, suggesting its specification must occur before the mid-blastula stage or be independent of the Wnt pathway. Thus, our experimental data suggests that disturbing *T. transversa* Wnt signaling affects the development of the mantle lobe and the morphology of the apical/mantle boundary, and that *pax6* might have an earlier upstream role in the embryonic body patterning of brachiopods.

Candidate genes are not iterated through all four partitions of *N. anomala* mesoderm

While there is little evidence for body wall segmentation in larval brachiopods, the mesoderm of *N. anomala* is clearly divided into four pairs of coelomic sacs. Do any of the genes correlate with its mesoderm segmentation? Expression of *en* borders the posterior boundary of coelomic sacs in the mesoderm of *N. anomala*. However, these mesodermal domains are only detected in the second and third coelomic sacs. Interestingly, the mesodermal domains initiate adjacent to the preceding ectodermal domains of *en* suggesting the ectoderm might signal to the mesoderm during brachiopod development. Thus, *en* expression is compatible with a segmentation role only in two out of four coeloms of the mesoderm of *N. anomala*. In fact, none of the other genes expressed in the mesoderm of *N. anomala* (*pax2/5/8*, *ptc*, *smo* and *gli*) show iterated patterns throughout the four coelomic sacs. In addition, *en*, *ptc*, *smo* and *gli*, but not *pax2/5/8*, are also expressed in the unsegmented mesoderm of *T. transversa* indicating that it is premature to assume a segmentation role for these genes in the mesoderm of *N. anomala*. How does the gene expression in the mesoderm of *N. anomala* compare to the segmented mesoderm of other animals?

Expression of *en* in annelids is restricted to mesodermal patches and does not resemble the patterns in brachiopods (Prud'homme *et al.* 2003; Seaver & Kaneshige 2006). Even though, in both brachiopods and annelids, *en* expression in the mesoderm seems to be connected to the *en* expression in the ectoderm (Seaver & Kaneshige 2006). Expression of *en* in *N. anomala* mesoderm, despite not being repeated, is similar to the more distantly related amphioxus (Holland *et al.* 1997) and onychophorans (Eriksson *et al.* 2009; Wedeen *et al.* 1997) with *en* expression localized to the posterior portion of mesodermal somites. However, the actual role of a posterior *en* domain in the

bioRxiv preprint doi: https://doi.org/10.1101/029892; this version posted January 25, 2016. The copyright holder for this preprint (which was not certified by peer review) is the author/funder, who has granted bioRxiv a license to display the preprint in perpetuity. It is made available under aCC-BY 4.0 International license.

mesoderm is unknown and requires further investigation in these animals. In contrast, the role of *en* in the body wall segmentation has been thoroughly studied.

Gene expression does not support a typical segment polarity role in brachiopods

Segment polarity genes are the hallmark of arthropod segmentation. We investigated whether the expression of *en*, *wnt1* and *hh* orthologs in brachiopods is compatible with a putative segment polarity role. The parasegment of arthropods is characterized by a cell population expressing *en* and *hh* adjacent to an anterior cell population expressing *wnt1*, *ptc*, *smo* and *gli* (Figure 9C). This stands in contrast to brachiopods where transcripts of *hh* are not detected in *en*-expressing cells, and *ptc*, *smo*, and *gli* are not coexpressed with *wnt1* at any developmental stage (Figure 9C). Thus, these differences in the gene expression do not support the presence of a typical segment polarity role in larval brachiopods.

On the other hand, we made the striking observation that *en* and *wnt1* are expressed as adjacent stripes demarcating the apical/mantle furrow of the brachiopod *T. transversa*. Such spatial arrangement is not only a characteristic feature of *D. melanogaster* parasegments, but a well conserved pattern in the segmentation of other arthropods (Damen 2007; Hughes & Kaufman 2002; Mellenthin *et al.* 2006; Nagy 1994). Remarkably, the adjacent expression of *en* and *wnt1* also demarcates the segment boundaries of one annelid, *P. dumerilii* (Prud'homme *et al.* 2003). It was suggested that this similarity reflects an evolutionary conservation of segmentation supporting the homology between annelid segments and arthropod parasegments (Prud'homme *et al.* 2003). However, distinguishing homology from convergence requires the recovery of the ancestral character state for each group, which in turn requires the comparative analysis of ingroup variability. While *en* and *wnt1* have a conserved role in arthropod segmentation, the expression of segment polarity genes in annelids is more variable and does not support a role in segment formation (Seaver 2003).

First, the spatial relationship of *en* expression and segment boundaries differs between species. It occurs at the posterior portion of segments in the leech *Helobdella triserialis* (Lans *et al.* 1993; Wedeen & Weisblat 1991) and *Capitella teleta* (Seaver & Kaneshige 2006), at the anterior portion in *P. dumerilii* (Prud'homme *et al.* 2003) and *Chaetopterus* sp. (Seaver *et al.* 2001), and not associated with segments in *Hydroides elegans* (Seaver & Kaneshige 2006) and *Pristina leidyi* (Bely & Wray 2001). Second, *en* expression can be restricted to individual cells (Bely & Wray 2001; Lans *et al.* 1993; Wedeen & Weisblat 1991), discontinuous patches (Seaver & Kaneshige 2006) or fuller stripes lining the segment boundary (Prud'homme *et al.* 2003); only the latter supporting a role in segment formation. Third, the temporal relationship of *en* expression and the morphological segmentation varies, and only in *P. dumerilii* and *C. teleta* is *en* expressed in stripes before the morphology is visible (Prud'homme *et al.* 2003; Seaver & Kaneshige 2006). In fact, with the exception of *P. dumerilii* (Dray *et al.* 2010; Prud'homme *et al.* 2003), the expression of *en* is not compatible with a segmentation role in most annelids investigated so far, *i.e.*, the leech *H. triserialis* (Lans *et al.* 1993; Seaver & Shankland 2001; Wedeen & Weisblat 1991), *P. leidyi* (Bely & Wray 2001), *Chaetopterus* sp. (Seaver *et al.* 2001), *C. teleta* and *H. elegans* (Seaver & Kaneshige 2006).

Expression of other segment polarity genes in annelids is much less known but still inconsistent between species. In *P. dumerilii*, expression of both *wnt1* and *hh* supports a role in segment formation (Dray *et al.* 2010; Prud'homme *et al.* 2003). In contrast,

bioRxiv preprint doi: https://doi.org/10.1101/029892; this version posted January 25, 2016. The copyright holder for this preprint (which was not certified by peer review) is the author/funder, who has granted bioRxiv a license to display the preprint in perpetuity. It is made available under aCC-BY 4.0 International license.

data from the only other annelid where *wnt1* has been investigated does not support a role in segmentation (Seaver & Kaneshige 2006). Expression of *hh* is also not compatible with a segmentation role in *Helobdella robusta* (Kang *et al.* 2003) or *C. teleta* (Seaver & Kaneshige 2006). Therefore, expression of segment polarity genes is variable even within the homologous segments of annelids. For this reason, the ancestral character state regarding the expression of *en*, *wnt1* and *hh* in annelids and their relation to segmentation remains unresolved.

In summary, the expression of segment polarity genes is greatly conserved in arthropods, but variable in annelids and brachiopods (inconsistent *wnt1* expression between *T. transversa* and *N. anomala*). This variation weakens the idea that segment polarity genes had an ancestral segmentation role in annelids and renders uncertain if *wnt1* was expressed at the apical/mantle boundary of a brachiopod ancestor. It suggests the adjacent expression of *en* and *wnt1* might be a convergent pattern between one annelid (*P. dumerilii*) and one brachiopod (*T. transversa*). However, additional data in annelids are needed to recover the ancestral state for the expression of *wnt1* and *hh* and maybe expose the developmental basis for the recurrent evolution of segment polarity like patterns. In any case, we show that abutting stripes of *en* and *wnt1* are not exclusive for the body segmentation of annelids and arthropods—it also occurs in a nonsegmental boundary of a larval brachiopod. The similarities can reflect the homology of developmental mechanisms of boundary formation, not linked to segmentation, or simply the cooption of an ancestral molecular network to various developmental boundaries.

Ancestral expression of *engrailed* was nonsegmental

As discussed above, *wnt1* expression is variable in the studied brachiopod species. If we strictly consider the genes with consistent expression (*i.e.*, *pax6*, *pax2/5/8* and *en*), the apical/mantle boundary of brachiopods is more similar to a vertebrate brain boundary than to an annelid segment boundary. In the vertebrate brain an anterior domain of *pax6* initially overlaps with the more posterior expression of *pax2/5/8* and *en* and defines the position of the di/mesencephalon boundary by mutual repression (Araki & Nakamura 1999; Matsunaga *et al.* 2000). The spatial correlation of these genes regarding the apical/mantle furrow of brachiopods is similar to the patterns defining the di/mesencephalon boundary (Figure 9B). Since there is no morphological evidence that a vertebrate brain is homologous to brachiopod larval lobes, this similarity in gene expression is likely the result of convergent evolution. In protostomes, even though *pax6* is recurrently associated to anterior structures, the expression of *pax2/5/8* is variable and not complementary to *pax6* (Additional file 4: Table S1). However, data on the expression of *pax6* and *pax2/5/8* are still scarce outside arthropods and it is unclear if the brachiopod pattern is ancestral to protostomes. In contrast, the complementary patterns of *pax6* and *pax2/5/8* expression occur in the ectoderm of hemichordates (Pani *et al.* 2012) and cephalochordates (Glardon *et al.* 1998; Kozmik *et al.* 1999) suggesting this is a conserved feature of deuterostomes. In fact, deuterostomes share a similar arrangement of gene products along the anteroposterior axis, a feature likely conserved in their last common ancestor (Lowe *et al.* 2015). Thus, if bilaterians had a conserved molecular cassette related to the patterning of the anteroposterior axis, such genes could have become associated to the various morphological structures evolved within each lineage and been independently recruited to similar developmental roles.

bioRxiv preprint doi: https://doi.org/10.1101/029892; this version posted January 25, 2016. The copyright holder for this preprint (which was not certified by peer review) is the author/funder, who has granted bioRxiv a license to display the preprint in perpetuity. It is made available under aCC-BY 4.0 International license.

We consider the idea above by reviewing the expression of *en*, a gene more widely studied across bilaterians. The comparison reveals the majority of groups have bilateral or dorsal domains of *en* in the ectoderm as its earliest instance of embryonic expression (Figure 10). Interestingly, many domains correlate to some kind of epithelial boundary such as the apical/mantle boundary of larval brachiopods, head/trunk and segment boundaries of annelids, shell borders in molluscs, arthropod head/trunk and segment boundaries, seam cells in nematodes, collar/trunk boundary in hemichordates, brain boundaries in vertebrates and somite boundaries in cephalochordates (Additional file 4: Table S1). Such data indicates that the last common bilaterian ancestor had *en* expressed during early embryogenesis and that these homologous domains became associated to a variety of developmental boundaries. Can we identify the ancestral character state for the expression of *en* in bilaterians?

Annelids and brachiopods share a pair of lateral *en* domains that localize to the head/trunk and apical/mantle boundary, respectively. In *D. melanogaster* the first stripe of *en* occurs at the cephalic furrow (Fjose *et al.* 1985) and in hemichordates *en* is expressed at the collar/trunk boundary (Pani *et al.* 2012). Thus, comparative data suggests that *en* might have been associated to the interface between an anterior (*e.g.*, head) and a posterior region of the embryo (*e.g.*, trunk), a division shared by most bilaterians. From this ancestral embryonic domain(s), *en* was coopted independently to trunk segmentation in the arthropod parasegments, annelid segments, brachiopod larval boundaries and other developmental boundaries. This phenomenon can explain the mosaic of similarities and differences between gene expression and morphological characters in the Bilateria. Nevertheless, testing this idea requires the resolution of the basal bilaterian relationships to clarify the ancestral morphological characters as well as comparative gene expression studies in a number of other protostomes like gastrotrichs, rotifers, chaetognaths, nemerteans and priapulids. Only then will we have better support to establish the ancestral character states for each lineage and understand the interplay between molecular pathways and morphological characters during animal evolution. It is important to note that the homology of *en* domains during the early embryogenesis of bilaterians suggested by comparative data, does not imply the conservation of *en* function in boundary development. Thus, ancestral homologous domains might have functionally diverged within the different morphological contexts of Bilateria.

Conclusions

In conclusion, we show that a fine-grained comparative approach is crucial to distinguish ancestral and derived traits. Brachiopods have a conserved expression of *pax6*, *pax2/5/8* and *en*, which correlates to the morphology at the apical/mantle boundary. We found that a nonsegmental ectodermal boundary can express *en* and *wnt1* similarly to arthropod parasegments and that this might be a convergent pattern. In addition, a comparative analysis suggests the ancestral bilaterian had a pair of *en* domains that were coopted to different developmental boundaries during evolution. Therefore, arthropods and annelids might have independently recruited pre-existing boundary formation mechanisms for body segmentation (Martindale & Hejnol 2009). This argumentation is supported by recent phylogenies with improved resolution in the Protostomia, which challenge the homology between annelid and arthropod segments, and suggest an spiralian ancestor without trunk segmentation (Laumer *et al.* 2015; Struck *et al.* 2014). Overall, gene expression data in a comparative phylogenetic context is a promising approach to deconstruct segmentation into more fundamental developmen-

bioRxiv preprint doi: https://doi.org/10.1101/029892; this version posted January 25, 2016. The copyright holder for this preprint (which was not certified by peer review) is the author/funder, who has granted bioRxiv a license to display the preprint in perpetuity. It is made available under aCC-BY 4.0 International license.

tal mechanisms and recover the evolutionary relationships between the great diversity of segmented structures of bilaterians.

Materials and methods

Sample collection

We collected adult brachiopods by dredging rocky ocean floor in Friday Harbor, USA (*T. transversa*) and Raunefjorden near Bergen, Norway (*N. anomala*) during reproductive season, January and September/October respectively. Fertilization of ripe gametes was conducted in the laboratory as described previously (Freeman 1993, 2000) and the representative developmental stages were fixed in 4% formaldehyde for 1h, washed in PTw (1x PBS + 0.1% Tween-20) and kept in PTw at 4°C for antibody staining and in 100% methanol at -20°C for *in situ* hybridization.

Immunohistochemistry

We permeabilized the embryos with several washes in PTx (1x PBS + 0.2% Triton X-100) for 2h and blocked with two washes of 1h in PTx + 0.1% BSA (Bovine Serum Albumin) succeeded by 1h incubation in PTx + 5% NGS (Normal Goat Serum). Samples were incubated with the primary antibodies (mouse anti-Tyrosinated Tubulin 1:500 and rabbit anti-Synapsin II 1:500) stored overnight at 4°C on a nutator. We removed the primary antibodies with three 5 min and four 30 min washes in PTx + 0.1% BSA, blocked in PTx + 5% NGS for 1h and incubated nutating overnight at 4°C with the secondary antibodies (Alexa Fluor 594 anti-mouse and Alexa Fluor 647 anti-rabbit 1:200). Secondary antibodies were removed with three 5 min followed by several washes in PTx + 0.1% BSA for 2h. We stained nuclei by incubating permeabilized embryos in DAPI 1:500 or Sytox Green 1:1000 for 2h. Nuclei staining was combined with f-actin staining by the addition of BODIPY FL Phallacidin 5 U/mL previously evaporated to remove methanol.

Gene cloning and orthology

We identified orthologous genes by reciprocal BLAST searches using known sequences against the transcriptomes of *T. transversa* and *N. anomala*. We performed PCR gene specific primer pairs on cDNA of each brachiopod species synthesized with the SMARTer RACE cDNA Amplification kit (Clontech). We used RACE primers to clone *T. transversa en* and *pax6*. All other *T. transversa* (Ttra) and *N. anomala* (Nano) genes were cloned with regular primer pairs (Additional file 5: Table S2).

Primers were designed with Primer3 (Untergasser *et al.* 2012). Orthology was assigned by aligning amino acid sequences of brachiopods against annotated genes using MAFFT 7.215 (Katoh & Standley 2013), retaining only informative portions of the alignment with GBlocks 0.91b with relaxed parameters (Talavera & Castresana 2007) and running a Maximum Likelihood phylogenetic analysis with RAxML 8.1.17 (Stamatakis 2014) using automatic model recognition and rapid bootstrap (Additional file 6: Figure S4).

Alignments were manually verified using UGENE (Okonechnikov *et al.* 2012). Resulting trees from the maximum likelihood analysis were rendered into cladograms using the ETE Toolkit (Huerta-Cepas *et al.* 2010). Source files, alignments and scripts are available online (Vellutini & Hejnol 2015).

bioRxiv preprint doi: https://doi.org/10.1101/029892; this version posted January 25, 2016. The copyright holder for this preprint (which was not certified by peer review) is the author/funder, who has granted bioRxiv a license to display the preprint in perpetuity. It is made available under aCC-BY 4.0 International license.

In situ hybridization

We synthesized antisense DIG-labeled riboprobes with MEGAscript kit (Ambion) and performed colorimetric *in situ* hybridization according to an established protocol (Martín-Durán *et al.* 2012). Whole mount double fluorescent *in situ* hybridization was performed with the above protocol, but hybridizing the samples with a DIG-labeled and a DNP-labeled riboprobes. Samples were first incubated overnight at 4°C with Anti-DIG-POD conjugate diluted 1:250 in blocking buffer. After PTw washes, we developed the reaction with the TSA reagent kit Cy3 (Perkin Elmer). POD activity was inactivated by incubating 45 min in 0.1% H_2O_2 in PTw at room temperature followed by a 15 min incubation at 67°C in a detergent solution (50% formamide, 2x SSC, 1% SDS) and incubated overnight at 4°C with Anti-DNP-POD conjugate diluted 1:100 in blocking buffer. Second probe was developed in the same manner with the TSA reagent kit Cy5 (PerkinElmer).

Imaging and image processing

Specimens were mounted in 80% Glycerol in PBS, 97% 2,2'-Thiodiethanol (Asadulina *et al.* 2012; Staudt *et al.* 2007) or Murray's Clear (2:1 benzyl benzoate and benzyl alcohol solution) after a quick dehydration series in isopropanol (70%, 85%, 95%, 100%). After colorimetric *in situ* hybridization we imaged samples with a Zeiss AxioCam HRc mounted on a Zeiss Axioscope A1 using differential interference contrast technique (Nomarski). Fluorescent in situ hybridization and immunostainings were imaged in a Confocal Leica TCS SP5 and the resulting confocal stacks were processed in Fiji (Schindelin *et al.* 2012). We adjusted the levels of the final panels to improve the contrast using Fiji for confocal stacks and GIMP for photomicrographs. We created vector graphics and assembled the figure plates using Inkscape.

Inhibitor experiments with 1-azakenpaullone

We sampled developing embryos of *T. transversa* from wild type cultures and incubated with a final concentration of 1 and 10 µM 1-azakenpaullone diluted in seawater. Embryos were picked at the mid-blastula and radial gastrula stage and fixed for immunohistochemistry and *in situ* hybridization at the bilateral gastrula and trilobed larval stage. Controls were treated with the highest concentration of dimethyl sulfoxide (DMSO) contained in the experimental samples, 1% DMSO in seawater.

Availability of supporting data

The dataset containing the source files, alignments and scripts for gene orthology inference are available in the fig**share** repository at http://dx.doi.org/10.6084/m9.figshare.1473087 (Vellutini & Hejnol 2015).

List of abbreviations

DMSO: dimethyl sulfoxide, PTw: 1x PBS + 0.1% Tween-20, PTx: 1x PBS + 0.2% Triton X-100, *en*: *engrailed*, *hh*: *hedgehog*, *ptc*: *patched*, *smo*: *smoothened*

Competing interests

The authors declare that they have no competing interests.

bioRxiv preprint doi: https://doi.org/10.1101/029892; this version posted January 25, 2016. The copyright holder for this preprint (which was not certified by peer review) is the author/funder, who has granted bioRxiv a license to display the preprint in perpetuity. It is made available under aCC-BY 4.0 International license.

Authors' contributions

BCV and AH designed the study. BCV performed the experiments and analyzed the data. BCV and AH and wrote the manuscript. Both authors read and approved the final manuscript.

Acknowledgements

We thank Chema Martín-Durán for crucial discussions and help with in situ hybridization experiments, Carmen Andrikou and Kevin Pang for improving the manuscript, all members of S9 Lab for continuous support, and the staff of Friday Harbor Labs and Espeland Marine Biological Station for the help with collections. Alessandro Minelli for comments on an earlier draft. The study was funded by the core budget of the Sars Centre and received support from the Meltzer Research Fund.

bioRxiv preprint doi: https://doi.org/10.1101/029892; this version posted January 25, 2016. The copyright holder for this preprint (which was not certified by peer review) is the author/funder, who has granted bioRxiv a license to display the preprint in perpetuity. It is made available under aCC-BY 4.0 International license.

References

Abouheif, E., Akam, M., Dickinson, W.J., Holland, P.W., Meyer, A., Patel, N.H., Raff, R.A., Roth, V.L. & Wray, G.A. (1997) Homology and developmental genes. *Trends Genet.* 13, 432–433.

Ahzhanov, A. & Kaufman, T.C. (2000) Evolution of distinct expression patterns for *engrailed* paralogues in higher crustaceans (Malacostraca). *Dev. Genes Evol.* 210, 493–506.

Araki, I. & Nakamura, H. (1999) *Engrailed* defines the position of dorsal di-mesencephalic boundary by repressing diencephalic fate. *Development* 126, 5127–5135.

Arendt, D., Tessmar, K., Campos-Baptista, M.-I.M. de, Dorresteijn, A. & Wittbrodt, J. (2002) Development of pigment-cup eyes in the polychaete *Platynereis dumerilii* and evolutionary conservation of larval eyes in Bilateria. *Development* 129, 1143–1154.

Asadulina, A., Panzera, A., Verasztó, C., Liebig, C. & Jékely, G. (2012) Whole-body gene expression pattern registration in *Platynereis* larvae. *Evodevo* 3, 27.

Balavoine, G. & Adoutte, A. (2003) The segmented *Urbilateria*: A testable scenario. *Integr. Comp. Biol.* 43, 137–147.

Balfour, F.M. (1880) *A treatise on comparative embryology*. Macmillan; Company.

Baratte, S., Andouche, A. & Bonnaud, L. (2007) *Engrailed* in cephalopods: A key gene related to the emergence of morphological novelties. *Dev. Genes Evol.* 217, 353–362.

Bassham, S., Cañestro, C. & Postlethwait, J.H. (2008) Evolution of developmental roles of *Pax2/5/8* paralogs after independent duplication in urochordate and vertebrate lineages. *BMC Biol.* 6, 35.

Bely, A.E. & Wray, G.A. (2001) Evolution of regeneration and fission in annelids: Insights from *engrailed*- and *orthodenticle*-class gene expression. *Development* 128, 2781–2791.

Bitner, M.A. & Cohen, B.L. (2013) Brachiopoda. In: *eLS*. John Wiley & Sons, Ltd.

Boell, L.A. & Bucher, G. (2008) Whole-mount in situ hybridization in the rotifer *Brachionus plicatilis* representing a basal branch of lophotrochozoans. *Dev. Genes Evol.* 218, 445–451.

Brivanlou, A.H. & Harland, R.M. (1989) Expression of an *engrailed*-related protein is induced in the anterior neural ectoderm of early *Xenopus* embryos. *Development* 106, 611–617.

Brown, S.J., Patel, N.H. & Denell, R.E. (1994) Embryonic expression of the single *Tribolium engrailed* homolog. *Dev. Genet.* 15, 7–18.

Budd, G.E. (2001) Why are arthropods segmented? *Evol. Dev.* 3, 332–342.

Byrne, M., Cisternas, P.A., Elia, L. & Relf, B. (2005) *Engrailed* is expressed in larval development and in the radial nervous system of *Patiriella* sea stars. *Dev. Genes Evol.* 215, 608–617.

bioRxiv preprint doi: https://doi.org/10.1101/029892; this version posted January 25, 2016. The copyright holder for this preprint (which was not certified by peer review) is the author/funder, who has granted bioRxiv a license to display the preprint in perpetuity. It is made available under aCC-BY 4.0 International license.

Cadigan, K.M., Grossniklaus, U. & Gehring, W.J. (1994) Localized expression of *sloppy paired* protein maintains the polarity of *Drosophila* parasegments. *Genes Dev.* 8, 899–913.

Callaerts, P., Munoz-Marmol, A.M., Glardon, S., Castillo, E., Sun, H., Li, W.-H., Gehring, W.J. & Salo, E. (1999) Isolation and expression of a *Pax-6* gene in the regenerating and intact Planarian *Dugesia(G)tigrina*. *Proceedings of the National Academy of Sciences* 96, 558–563.

Cañestro, C., Bassham, S. & Postlethwait, J. (2005) Development of the central nervous system in the larvacean *Oikopleura dioica* and the evolution of the chordate brain. *Dev. Biol.* 285, 298–315.

Cassata, G., Shemer, G., Morandi, P., Donhauser, R., Podbilewicz, B. & Baumeister, R. (2005) *Ceh-16/engrailed* patterns the embryonic epidermis of *Caenorhabditis elegans*. *Development* 132, 739–749.

Chipman, A.D. (2010) Parallel evolution of segmentation by co-option of ancestral gene regulatory networks. *Bioessays* 32, 60–70.

Chisholm, A.D. & Horvitz, H.R. (1995) Patterning of the *Caenorhabditis elegans* head region by the *Pax-6* family member *vab-3*. *Nature* 377, 52–55.

Conklin, E.G. (1902) The embryology of a brachiopod, *Terebratulina septentrionalis* Couthouy. *Proc. Am. Philos. Soc.* 41, 41–76.

Czerny, T., Bouchard, M., Kozmik, Z. & Busslinger, M. (1997) The characterization of novel *Pax* genes of the sea urchin and *Drosophila* reveal an ancient evolutionary origin of the *Pax2/5/8* subfamily. *Mech. Dev.* 67, 179–192.

Dahmann, C., Oates, A.C. & Brand, M. (2011) Boundary formation and maintenance in tissue development. *Nat. Rev. Genet.* 12, 43–55.

Damen, W.G.M. (2002) Parasegmental organization of the spider embryo implies that the parasegment is an evolutionary conserved entity in arthropod embryogenesis. *Development* 129, 1239–1250.

Damen, W.G.M. (2007) Evolutionary conservation and divergence of the segmentation process in arthropods. *Dev. Dyn.* 236, 1379–1391.

Danielian, P.S. & McMahon, A.P. (1996) *Engrailed-1* as a target of the Wnt-1 signalling pathway in vertebrate midbrain development. *Nature* 383, 332–334.

Davis, C.A., Holmyard, D.P., Millen, K.J. & Joyner, A.L. (1991) Examining pattern formation in mouse, chicken and frog embryos with an *En*-specific antiserum. *Development* 111, 287–298.

Davis, G.K. & Patel, N.H. (1999) The origin and evolution of segmentation. *Trends Cell Biol.* 9, M68–72.

De Robertis, E.M. (1997) Evolutionary biology. The ancestry of segmentation. *Nature* 387, 25–26.

De Robertis, E.M. (2008) The molecular ancestry of segmentation mechanisms. *Proc. Natl. Acad. Sci. U. S. A.* 105, 16411–16412.

bioRxiv preprint doi: https://doi.org/10.1101/029892; this version posted January 25, 2016. The copyright holder for this preprint (which was not certified by peer review) is the author/funder, who has granted bioRxiv a license to display the preprint in perpetuity. It is made available under aCC-BY 4.0 International license.

Denes, A.S., Jékely, G., Steinmetz, P.R.H., Raible, F., Snyman, H., Prud'homme, B., Ferrier, D.E.K., Balavoine, G. & Arendt, D. (2007) Molecular architecture of annelid nerve cord supports common origin of nervous system centralization in Bilateria. *Cell* 129, 277–288.

Derobert, Y., Baratte, B., Lepage, M. & Mazan, S. (2002) *Pax6* expression patterns in *Lampetra fluviatilis* and *Scyliorhinus canicula* embryos suggest highly conserved roles in the early regionalization of the vertebrate brain. *Brain Res. Bull.* 57, 277–280.

DiNardo, S. & O'Farrell, P.H. (1987) Establishment and refinement of segmental pattern in the *Drosophila* embryo: Spatial control of *engrailed* expression by pair-rule genes. *Genes Dev.* 1, 1212–1225.

Dolecki, G.J. & Humphreys, T. (1988) An *engrailed* class homeo box gene in sea urchins. *Gene* 64, 21–31.

Dougan, S. & DiNardo, S. (1992) *Drosophila wingless* generates cell type diversity among *engrailed* expressing cells. *Nature* 360, 347–350.

Dray, N., Tessmar-Raible, K., Le Gouar, M., Vibert, L., Christodoulou, F., Schipany, K., Guillou, A., Zantke, J., Snyman, H., Béhague, J., Vervoort, M., Arendt, D. & Balavoine, G. (2010) Hedgehog signaling regulates segment formation in the annelid *Platynereis*. *Science* 329, 339–342.

Ekker, M., Wegner, J., Akimenko, M.A. & Westerfield, M. (1992) Coordinate embryonic expression of three zebrafish *engrailed* genes. *Development* 116, 1001–1010.

Eriksson, B.J., Samadi, L. & Schmid, A. (2013) The expression pattern of the genes *engrailed*, *pax6*, *otd* and *six3* with special respect to head and eye development in *Euperipatoides kanangrensis* Reid 1996 (Onychophora: Peripatopsidae). *Dev. Genes Evol.* 223, 237–246.

Eriksson, B.J., Tait, N.N., Budd, G.E. & Akam, M. (2009) The involvement of *engrailed* and *wingless* during segmentation in the onychophoran *Euperipatoides kanangrensis* (Peripatopsidae: Onychophora) (Reid 1996). *Dev. Genes Evol.* 219, 249–264.

Farzana, L. & Brown, S.J. (2008) Hedgehog signaling pathway function conserved in *Tribolium* segmentation. *Dev. Genes Evol.* 218, 181–192.

Fjose, A., McGinnis, W.J. & Gehring, W.J. (1985) Isolation of a homoeo box-containing gene from the *engrailed* region of *Drosophila* and the spatial distribution of its transcripts. *Nature* 313, 284–289.

Fleig, R. (1990) *Engrailed* expression and body segmentation in the honeybee *Apis mellifera*. *Rouxs. Arch. Dev. Biol.* 198, 467–473.

Franke, F.A. & Mayer, G. (2014) Controversies surrounding segments and parasegments in onychophora: Insights from the expression patterns of four "segment polarity genes" in the peripatopsid *Euperipatoides rowelli*. *PLoS One* 9, e114383.

Franke, F.A., Schumann, I., Hering, L. & Mayer, G. (2015) Phylogenetic analysis and expression patterns of *Pax* genes in the onychophoran *Euperipatoides rowelli* reveal a novel bilaterian *P*ax subfamily. *Evol. Dev.* 17, 3–20.

bioRxiv preprint doi: https://doi.org/10.1101/029892; this version posted January 25, 2016. The copyright holder for this preprint (which was not certified by peer review) is the author/funder, who has granted bioRxiv a license to display the preprint in perpetuity. It is made available under aCC-BY 4.0 International license.

Freeman, G. (1993) Regional specification during embryogenesis in the articulate brachiopod *Terebratalia*. *Dev. Biol.* 160, 196–213.

Freeman, G. (2000) Regional specification during embryogenesis in the craniiform brachiopod *Crania anomala*. *Dev. Biol.* 227, 219–238.

Fujioka, M., Yusibova, G.L., Patel, N.H., Brown, S.J. & Jaynes, J.B. (2002) The repressor activity of Even-skipped is highly conserved, and is sufficient to activate *engrailed* and to regulate both the spacing and stability of parasegment boundaries. *Development* 129, 4411–4421.

Gabriel, W.N. & Goldstein, B. (2007) Segmental expression of *Pax3/7* and *engrailed* homologs in tardigrade development. *Dev. Genes Evol.* 217, 421–433.

Glardon, S., Callaerts, P., Halder, G. & Gehring, W.J. (1997) Conservation of *Pax-6* in a lower chordate, the ascidian *Phallusia mammillata*. *Development* 124, 817–825.

Glardon, S., Holland, L.Z., Gehring, W.J. & Holland, N.D. (1998) Isolation and developmental expression of the amphioxus *Pax-6* gene (*AmphiPax-6*): Insights into eye and photoreceptor evolution. *Development* 125, 2701–2710.

Hannibal, R.L. & Patel, N.H. (2013) What is a segment? *Evodevo* 4, 35.

Hartmann, B., Lee, P.N., Kang, Y.Y., Tomarev, S., Couet, H.G. de & Callaerts, P. (2003) *Pax6* in the sepiolid squid *Euprymna scolopes*: Evidence for a role in eye, sensory organ and brain development. *Mech. Dev.* 120, 177–183.

Hatta, K., Bremiller, R., Westerfield, M. & Kimmel, C.B. (1991) Diversity of expression of *engrailed*-like antigens in zebrafish. *Development* 112, 821–832.

Heller, N. & Brändli, A.W. (1999) *Xenopus Pax-2/5/8* orthologues: Novel insights into *Pax* gene evolution and identification of *Pax-8* as the earliest marker for otic and pronephric cell lineages. *Dev. Genet.* 24, 208–219.

Hohagen, J., Herlitze, I. & Jackson, D.J. (2015) An optimised whole mount in situ hybridisation protocol for the mollusc *Lymnaea stagnalis*. *BMC Dev. Biol.* 15, 19.

Holland, L.Z., Kene, M., Williams, N.A. & Holland, N.D. (1997) Sequence and embryonic expression of the amphioxus *engrailed* gene (*AmphiEn*): The metameric pattern of transcription resembles that of its segment-polarity homolog in *drosophila*. *Development* 124, 1723–1732.

Holland, N.D., Holland, L.Z., Honma, Y. & Fujii, T. (1993) *Engrailed* expression during development of a lamprey, *Lampetra japonica*: A possible clue to homologies between agnathan and gnathostome muscles of the mandibular arch. *Dev. Growth Differ.* 35, 153–160.

Huerta-Cepas, J., Dopazo, J. & Gabaldón, T. (2010) ETE: A python Environment for Tree Exploration. *BMC Bioinformatics* 11, 24.

Hughes, C.L. & Kaufman, T.C. (2002) Exploring myriapod segmentation: The expression patterns of *even-skipped*, *engrailed*, and *wingless* in a centipede. *Dev. Biol.* 247, 47–61.

bioRxiv preprint doi: https://doi.org/10.1101/029892; this version posted January 25, 2016. The copyright holder for this preprint (which was not certified by peer review) is the author/funder, who has granted bioRxiv a license to display the preprint in perpetuity. It is made available under aCC-BY 4.0 International license.

Hyman, L.H. (1959) The lophophorate coelomates—Phylum brachiopoda. In: *The invertebrates: Smaller coelomate groups*. McGraw-Hill Book Company, Inc, New York, pp. 568.

Imai, K.S., Satoh, N. & Satou, Y. (2002) Region specific gene expressions in the central nervous system of the ascidian embryo. *Mech. Dev.* 119 Suppl 1, S275–7.

Ingham, P.W. (1991) Segment polarity genes and cell patterning within the *Drosophila* body segment. *Curr. Opin. Genet. Dev.* 1, 261–267.

Ingham, P.W. & Martinez Arias, A. (1992) Boundaries and fields in early embryos. *Cell* 68, 221–235.

Ingham, P.W., Baker, N.E. & Martinez-Arias, A. (1988) Regulation of segment polarity genes in the *Drosophila* blastoderm by *fushi tarazu* and *even skipped*. *Nature* 331, 73–75.

Jacobs, D.K., Wray, C.G., Wedeen, C.J., Kostriken, R., DeSalle, R., Staton, J.L., Gates, R.D. & Lindberg, D.R. (2000) Molluscan *engrailed* expression, serial organization, and shell evolution. *Evol. Dev.* 2, 340–347.

Jiang, D. & Smith, W.C. (2002) An ascidian *engrailed* gene. *Dev. Genes Evol.* 212, 399–402.

John A. Long and Stephen A. Stricker (1991) Brachiopoda. In: A. C. Giese, J. S. Pearse, and V. Pearse (Eds), *Reproduction of marine invertebrates: Echinoderms and lophophorates*. The Boxwood Press, Pacific Grove, California, pp. 47–84.

Joyner, A.L. (1996) *Engrailed*, *Wnt* and *Pax* genes regulate midbrain-hindbrain development. *Trends Genet.* 12, 15–20.

Kang, D., Huang, F., Li, D., Shankland, M., Gaffield, W. & Weisblat, D.A. (2003) A *hedgehog* homolog regulates gut formation in leech (*Helobdella*). *Development* 130, 1645–1657.

Katoh, K. & Standley, D.M. (2013) MAFFT multiple sequence alignment software version 7: Improvements in performance and usability. *Mol. Biol. Evol.* 30, 772–780.

Kimmel, C.B. (1996) Was urbilateria segmented? *Trends Genet.* 12, 329–331.

Kornberg, T., Sidén, I., O'Farrell, P. & Simon, M. (1985) The *engrailed* locus of *Drosophila*: In situ localization of transcripts reveals compartment-specific expression. *Cell* 40, 45–53.

Kozmik, Z., Holland, N.D., Kalousova, A., Paces, J., Schubert, M. & Holland, L.Z. (1999) Characterization of an amphioxus paired box gene, *AmphiPax2/5/8*: Developmental expression patterns in optic support cells, nephridium, thyroid-like structures and pharyngeal gill slits, but not in the midbrain-hindbrain boundary region. *Development* 126, 1295–1304.

Kunick, C., Lauenroth, K., Leost, M., Meijer, L. & Lemcke, T. (2004) 1-azakenpaullone is a selective inhibitor of glycogen synthase kinase-3 beta. *Bioorg. Med. Chem. Lett.* 14, 413–416.

Lans, D., Wedeen, C.J. & Weisblat, D.A. (1993) Cell lineage analysis of the expression of an *engrailed* homolog in leech embryos. *Development* 117, 857–871.

bioRxiv preprint doi: https://doi.org/10.1101/029892; this version posted January 25, 2016. The copyright holder for this preprint (which was not certified by peer review) is the author/funder, who has granted bioRxiv a license to display the preprint in perpetuity. It is made available under aCC-BY 4.0 International license.

Laumer, C.E., Bekkouche, N., Kerbl, A., Goetz, F., Neves, R.C., Sørensen, M.V., Kristensen, R.M., Hejnol, A., Dunn, C.W., Giribet, G. & Worsaae, K. (2015) Spiralian phylogeny informs the evolution of microscopic lineages. *Curr. Biol.* 25, 2000–2006.

Lowe, C.J. & Wray, G.A. (1997) Radical alterations in the roles of homeobox genes during echinoderm evolution. *Nature* 389, 718–721.

Lowe, C.J., Clarke, D.N., Medeiros, D.M., Rokhsar, D.S. & Gerhart, J. (2015) The deuterostome context of chordate origins. *Nature* 520, 456–465.

Lowe, C.J., Wu, M., Salic, A., Evans, L., Lander, E., Stange-Thomann, N., Gruber, C.E., Gerhart, J. & Kirschner, M. (2003) Anteroposterior patterning in hemichordates and the origins of the chordate nervous system. *Cell* 113, 853–865.

Manzanares, M., Marco, R. & Garesse, R. (1993) Genomic organization and developmental pattern of expression of the *engrailed* gene from the brine shrimp *Artemia*. *Development* 118, 1209–1219.

Manzanares, M., Williams, T.A., Marco, R. & Garesse, R. (1996) Segmentation in the crustacean *Artemia*: *Engrailed* staining studied with an antibody raised against the *Artemia* protein. *Rouxs. Arch. Dev. Biol.* 205, 424–431.

Marie, B. & Bacon, J.P. (2000) Two *engrailed*-related genes in the cockroach: Cloning, phylogenetic analysis, expression and isolation of splice variants. *Dev. Genes Evol.* 210, 436–448.

Martindale, M.Q. & Hejnol, A. (2009) A developmental perspective: Changes in the position of the blastopore during bilaterian evolution. *Dev. Cell* 17, 162–174.

Martinez Arias, A., Baker, N.E. & Ingham, P.W. (1988) Role of segment polarity genes in the definition and maintenance of cell states in the *Drosophila* embryo. *Development* 103, 157–170.

Martinez-Arias, A. & Lawrence, P.A. (1985) Parasegments and compartments in the *Drosophila* embryo. *Nature* 313, 639–642.

Martín-Durán, J.M., Janssen, R., Wennberg, S., Budd, G.E. & Hejnol, A. (2012) Deuterostomic development in the protostome *Priapulus caudatus*. *Curr. Biol.* 22, 2161–2166.

Matsunaga, E., Araki, I. & Nakamura, H. (2000) *Pax6* defines the di-mesencephalic boundary by repressing *En1* and *Pax2*. *Development* 127, 2357–2365.

McCauley, D.W. & Bronner-Fraser, M. (2002) Conservation of *Pax* gene expression in ectodermal placodes of the lamprey. *Gene* 287, 129–139.

Mellenthin, K., Fahmy, K., Ali, R.A., Hunding, A., Da Rocha, S. & Baumgartner, S. (2006) Wingless signaling in a large insect, the blowfly *Lucilia sericata*: A beautiful example of evolutionary developmental biology. *Dev. Dyn.* 235, 347–360.

Minelli, A. & Fusco, G. (2004) Evo-devo perspectives on segmentation: Model organisms, and beyond. *Trends Ecol. Evol.* 19, 423–429.

Moshel, S.M., Levine, M. & Collier, J.R. (1998) Shell differentiation and *engrailed* expression in the *Ilyanassa* embryo. *Dev. Genes Evol.* 208, 135–141.

Nagy, L.M. (1994) Insect segmentation. A glance posterior. *Curr. Biol.* 4, 811–814.

bioRxiv preprint doi: https://doi.org/10.1101/029892; this version posted January 25, 2016. The copyright holder for this preprint (which was not certified by peer review) is the author/funder, who has granted bioRxiv a license to display the preprint in perpetuity. It is made available under aCC-BY 4.0 International license.

Navet, S., Andouche, A., Baratte, S. & Bonnaud, L. (2009) *Shh* and *Pax6* have unconventional expression patterns in embryonic morphogenesis in *Sepia officinalis* (Cephalopoda). *Gene Expr. Patterns* 9, 461–467.

Nederbragt, A.J., Loon, A.E. van & Dictus, W.J.A.G. (2002) Expression of *Patella vulgata* orthologs of *engrailed* and *dpp-bMP2/4* in adjacent domains during molluscan shell development suggests a conserved compartment boundary mechanism. *Dev. Biol.* 246, 341–355.

Nielsen, C. (1991) The development of the brachiopod *Crania (Neocrania) anomala* (O. F. Müller) and its phylogenetic significance. *Acta Zool.* 72, 7–28.

Njølstad, P.R. & Fjose, A. (1988) Insitu hybridization patterns of zebrafish homeobox genes homologous to *Hox-2.1* and *En-2* of mouse. *Biochem. Biophys. Res. Commun.*

Okafuji, T., Funahashi, J. & Nakamura, H. (1999) Roles of *Pax-2* in initiation of the chick tectal development. *Brain Res. Dev. Brain Res.* 116, 41–49.

Okonechnikov, K., Golosova, O., Fursov, M. & UGENE team (2012) Unipro UGENE: A unified bioinformatics toolkit. *Bioinformatics* 28, 1166–1167.

Omori, A., Akasaka, K., Kurokawa, D. & Amemiya, S. (2011) Gene expression analysis of *Six3*, *Pax6*, and *Otx* in the early development of the stalked crinoid *Metacrinus rotundus*. *Gene Expr. Patterns* 11, 48–56.

O'Brien, E.K. & Degnan, B.M. (2003) Expression of *Pax258* in the gastropod statocyst: Insights into the antiquity of metazoan geosensory organs. *Evol. Dev.* 5, 572–578.

Pani, A.M., Mullarkey, E.E., Aronowicz, J., Assimacopoulos, S., Grove, E.A. & Lowe, C.J. (2012) Ancient deuterostome origins of vertebrate brain signalling centres. *Nature* 483, 289–294.

Passamaneck, Y.J., Furchheim, N., Hejnol, A., Martindale, M.Q. & Lüter, C. (2011) Ciliary photoreceptors in the cerebral eyes of a protostome larva. *Evodevo* 2, 6.

Patel, N.H. (2003) The ancestry of segmentation. *Dev. Cell* 5, 2–4.

Patel, N.H., Martin-Blanco, E., Coleman, K.G., Poole, S.J., Ellis, M.C., Kornberg, T.B. & Goodman, C.S. (1989) Expression of *engrailed* proteins in arthropods, annelids, and chordates. *Cell* 58, 955–968.

Petersen, C.P. & Reddien, P.W. (2009) Wnt signaling and the polarity of the primary body axis. *Cell* 139, 1056–1068.

Pfeffer, P.L., Gerster, T., Lun, K., Brand, M. & Busslinger, M. (1998) Characterization of three novel members of the zebrafish *Pax2/5/8* family: Dependency of *Pax5* and *Pax8* expression on the *Pax2.1* (*noi*) function. *Development* 125, 3063–3074.

Prud'homme, B., Rosa, R. de, Arendt, D., Julien, J.-F., Pajaziti, R., Dorresteijn, A.W.C., Adoutte, A., Wittbrodt, J. & Balavoine, G. (2003) Arthropod-like expression patterns of *engrailed* and *wingless* in the annelid *Platynereis dumerilii* suggest a role in segment formation. *Curr. Biol.* 13, 1876–1881.

Püschel, A.W., Gruss, P. & Westerfield, M. (1992) Sequence and expression pattern of *pax-6* are highly conserved between zebrafish and mice. *Development* 114, 643–651.

bioRxiv preprint doi: https://doi.org/10.1101/029892; this version posted January 25, 2016. The copyright holder for this preprint (which was not certified by peer review) is the author/funder, who has granted bioRxiv a license to display the preprint in perpetuity. It is made available under aCC-BY 4.0 International license.

Quigley, I.K., Xie, X. & Shankland, M. (2007) *Hau-Pax6A* expression in the central nervous system of the leech embryo. *Dev. Genes Evol.* 217, 459–468.

Quiring, R., Walldorf, U., Kloter, U. & Gehring, W.J. (1994) Homology of the *eyeless* gene of *Drosophila* to the *Small eye* gene in mice and *Aniridia* in humans. *Science* 265, 785–789.

Rajakumar, V. & Chamberlin, H.M. (2007) The *Pax2/5/8* gene *egl-38* coordinates organogenesis of the *C. elegans* egg-laying system. *Dev. Biol.* 301, 240–253.

Rhinn, M. & Brand, M. (2001) The midbrain–hindbrain boundary organizer. *Curr. Opin. Neurobiol.* 11, 34–42.

Santagata, S., Resh, C., Hejnol, A., Martindale, M.Q. & Passamaneck, Y.J. (2012) Development of the larval anterior neurogenic domains of *Terebratalia transversa* (Brachiopoda) provides insights into the diversification of larval apical organs and the spiralian nervous system. *Evodevo* 3, 3.

Schindelin, J., Arganda-Carreras, I., Frise, E., Kaynig, V., Longair, M., Pietzsch, T., Preibisch, S., Rueden, C., Saalfeld, S., Schmid, B., Tinevez, J.-Y., White, D.J., Hartenstein, V., Eliceiri, K., Tomancak, P. & Cardona, A. (2012) Fiji: An open-source platform for biological-image analysis. *Nat. Methods* 9, 676–682.

Scholpp, S., Lohs, C. & Brand, M. (2003) Engrailed and Fgf8 act synergistically to maintain the boundary between diencephalon and mesencephalon. *Development* 130, 4881–4893.

Scholtz, G. (2002) The articulata hypothesis – or what is a segment? *Org. Divers. Evol.* 2, 197–215.

Seaver, E.C. (2003) Segmentation: Mono- or polyphyletic? *Int. J. Dev. Biol.* 47, 583–595.

Seaver, E.C. & Kaneshige, L.M. (2006) Expression of 'segmentation' genes during larval and juvenile development in the polychaetes *Capitella* sp. i and *H. elegans*. *Dev. Biol.* 289, 179–194.

Seaver, E.C. & Shankland, M. (2001) Establishment of segment polarity in the ectoderm of the leech *Helobdella*. *Development* 128, 1629–1641.

Seaver, E.C., Paulson, D.A., Irvine, S.Q. & Martindale, M.Q. (2001) The spatial and temporal expression of *Ch-en*, the *engrailed* gene in the polychaete *Chaetopterus*, does not support a role in body axis segmentation. *Dev. Biol.* 236, 195–209.

Shubin, N., Tabin, C. & Carroll, S.B. (2009) Deep homology and the origins of evolutionary novelty. *Nature* 457, 818–823.

Stamatakis, A. (2014) RAxML version 8: A tool for phylogenetic analysis and post-analysis of large phylogenies. *Bioinformatics* 30, 1312–1313.

Staudt, T., Lang, M.C., Medda, R., Engelhardt, J. & Hell, S.W. (2007) 2,2'-thiodiethanol: A new water soluble mounting medium for high resolution optical microscopy. *Microsc. Res. Tech.* 70, 1–9.

Struck, T.H., Wey-Fabrizius, A.R., Golombek, A., Hering, L., Weigert, A., Bleidorn, C., Klebow, S., Iakovenko, N., Hausdorf, B., Petersen, M., Kück, P., Herlyn, H. &

bioRxiv preprint doi: https://doi.org/10.1101/029892; this version posted January 25, 2016. The copyright holder for this preprint (which was not certified by peer review) is the author/funder, who has granted bioRxiv a license to display the preprint in perpetuity. It is made available under aCC-BY 4.0 International license.

Hankeln, T. (2014) Platyzoan paraphyly based on phylogenomic data supports a non-coelomate ancestry of Spiralia. *Mol. Biol. Evol.* 31, 1833–1849.

Tabata, T. & Kornberg, T.B. (1994) Hedgehog is a signaling protein with a key role in patterning *Drosophila* imaginal discs. *Cell* 76, 89–102.

Talavera, G. & Castresana, J. (2007) Improvement of phylogenies after removing divergent and ambiguously aligned blocks from protein sequence alignments. *Syst. Biol.* 56, 564–577.

Tarpin, M., Gehring, W.J. & Bièrne, J. (1999) Reverse homeosis in homeotically reconstructed ribbonworms. *Proc. Natl. Acad. Sci. U. S. A.* 96, 11900–11903.

Tautz, D. (2004) Segmentation. *Dev. Cell* 7, 301–312.

Temereva, E.N. & Malakhov, V.V. (2011) The evidence of metamery in adult brachiopods and phoronids. *Invert Zool* 8, 91–112.

Tomarev, S.I., Callaerts, P., Kos, L., Zinovieva, R., Halder, G., Gehring, W. & Piatigorsky, J. (1997) Squid Pax-6 and eye development. *Proc. Natl. Acad. Sci. U. S. A.* 94, 2421–2426.

Untergasser, A., Cutcutache, I., Koressaar, T., Ye, J., Faircloth, B.C., Remm, M. & Rozen, S.G. (2012) Primer3–new capabilities and interfaces. *Nucleic Acids Res.* 40, e115–e115.

Vellutini, B.C. & Hejnol, A. (2015) Gene orthology for the brachiopod segmentation project.

Wada, H., Saiga, H., Satoh, N. & Holland, P.W. (1998) Tripartite organization of the ancestral chordate brain and the antiquity of placodes: Insights from ascidian *Pax-2/5/8*, *Hox* and *Otx* genes. *Development* 125, 1113–1122.

Walther, C. & Gruss, P. (1991) *Pax-6*, a murine paired box gene, is expressed in the developing CNS. *Development* 113, 1435–1449.

Wanninger, A. & Haszprunar, G. (2001) The expression of an engrailed protein during embryonic shell formation of the tusk-shell, *Antalis entalis* (mollusca, scaphopoda). *Evolution and Development* 3, 312–321.

Wedeen, C.J. & Weisblat, D.A. (1991) Segmental expression of an *engrailed*-class gene during early development and neurogenesis in an annelid. *Development* 113, 805–814.

Wedeen, C.J., Kostriken, R.G., Leach, D. & Whitington, P. (1997) Segmentally iterated expression of an *engrailed*-class gene in the embryo of an australian onychophoran. *Dev. Genes Evol.* 207, 282–286.

Whitington, P.M., Meier, T. & King, P. (1991) Segmentation, neurogenesis and formation of early axonal pathways in the centipede, *Ethmostigmus rubripes* (Brandt). *Rouxs. Arch. Dev. Biol.* 199, 349–363.

Wollesen, T., Rodríguez Monje, S.V., Todt, C., Degnan, B.M. & Wanninger, A. (2015) Ancestral role of *pax2/5/8* in molluscan brain and multimodal sensory system development. *BMC Evol. Biol.* 15, 231.

bioRxiv preprint doi: https://doi.org/10.1101/029892; this version posted January 25, 2016. The copyright holder for this preprint (which was not certified by peer review) is the author/funder, who has granted bioRxiv a license to display the preprint in perpetuity. It is made available under aCC-BY 4.0 International license.

Yaguchi, S., Nakajima, Y., Wang, D. & Burke, R.D. (2006) Embryonic expression of *engrailed* in sea urchins. *Gene Expr. Patterns* 6, 566–571.

bioRxiv preprint doi: https://doi.org/10.1101/029892; this version posted January 25, 2016. The copyright holder for this preprint (which was not certified by peer review) is the author/funder, who has granted bioRxiv a license to display the preprint in perpetuity. It is made available under aCC-BY 4.0 International license.

Figures

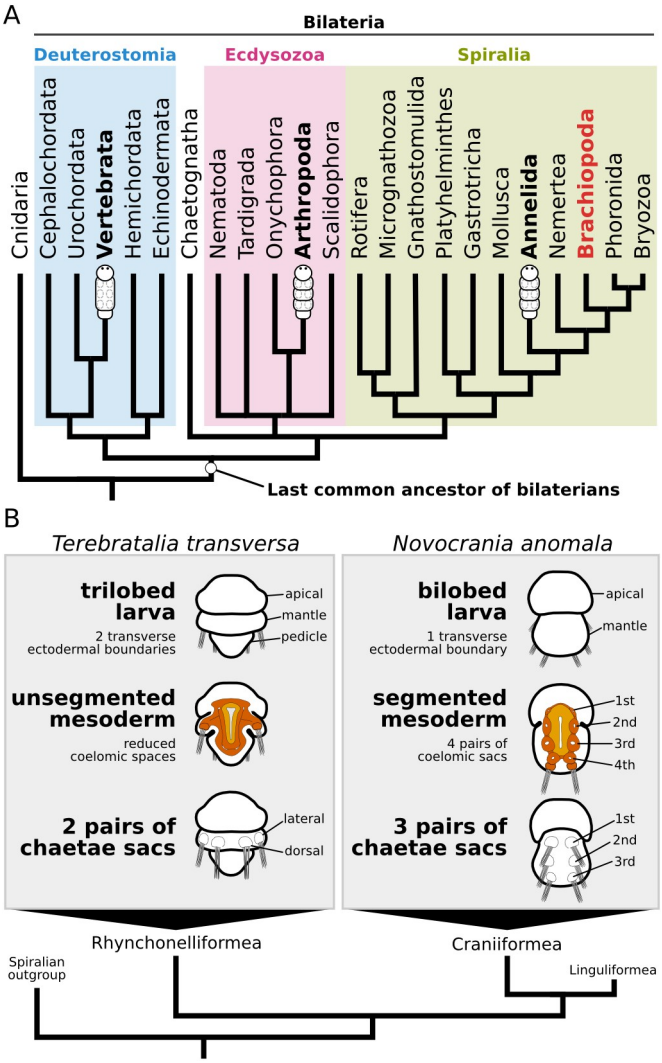

Figure 1. Phylogenetic relationships between bilaterally symmetrical animals and the morphological features of larval brachiopods. (A) Phylogenetic tree showing the three major bilaterian clades, Deuterostomia, Ecdysozoa and Spiralia. Animal groups regarded as truly segmented are marked in bold. The lineage of brachiopods is marked in red. Tree based on (Laumer *et al.* 2015). (B) Putative segmented traits of the larvae of the brachiopods *T. transversa* and *N. anomala*. Tree based on (Bitner & Cohen 2013).

bioRxiv preprint doi: https://doi.org/10.1101/029892; this version posted January 25, 2016. The copyright holder for this preprint (which was not certified by peer review) is the author/funder, who has granted bioRxiv a license to display the preprint in perpetuity. It is made available under aCC-BY 4.0 International license.

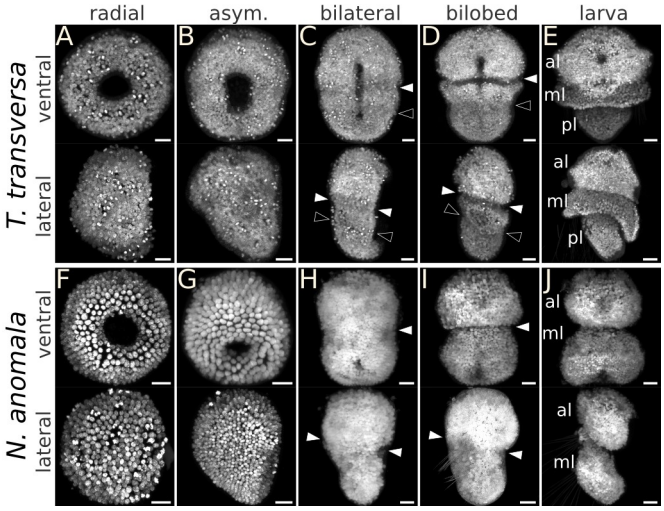

Figure 2. Developmental stages of the trilobed larva of *T. transversa* (A–E) and the bilobed larva of *N. anomala* (F–J). Each panel shows a ventral view (top) and lateral view (bottom) of a maximum intensity projection of embryos stained with DAPI. Anterior is top in all panels and ventral is to the right in all lateral views. White arrowheads mark the apical/mantle boundary and black arrowheads mark the mantle/pedicle boundary. al: apical lobe, ml: mantle lobe, pl: pedicle lobe. Scale bars = 20 µm.

bioRxiv preprint doi: https://doi.org/10.1101/029892; this version posted January 25, 2016. The copyright holder for this preprint (which was not certified by peer review) is the author/funder, who has granted bioRxiv a license to display the preprint in perpetuity. It is made available under aCC-BY 4.0 International license.

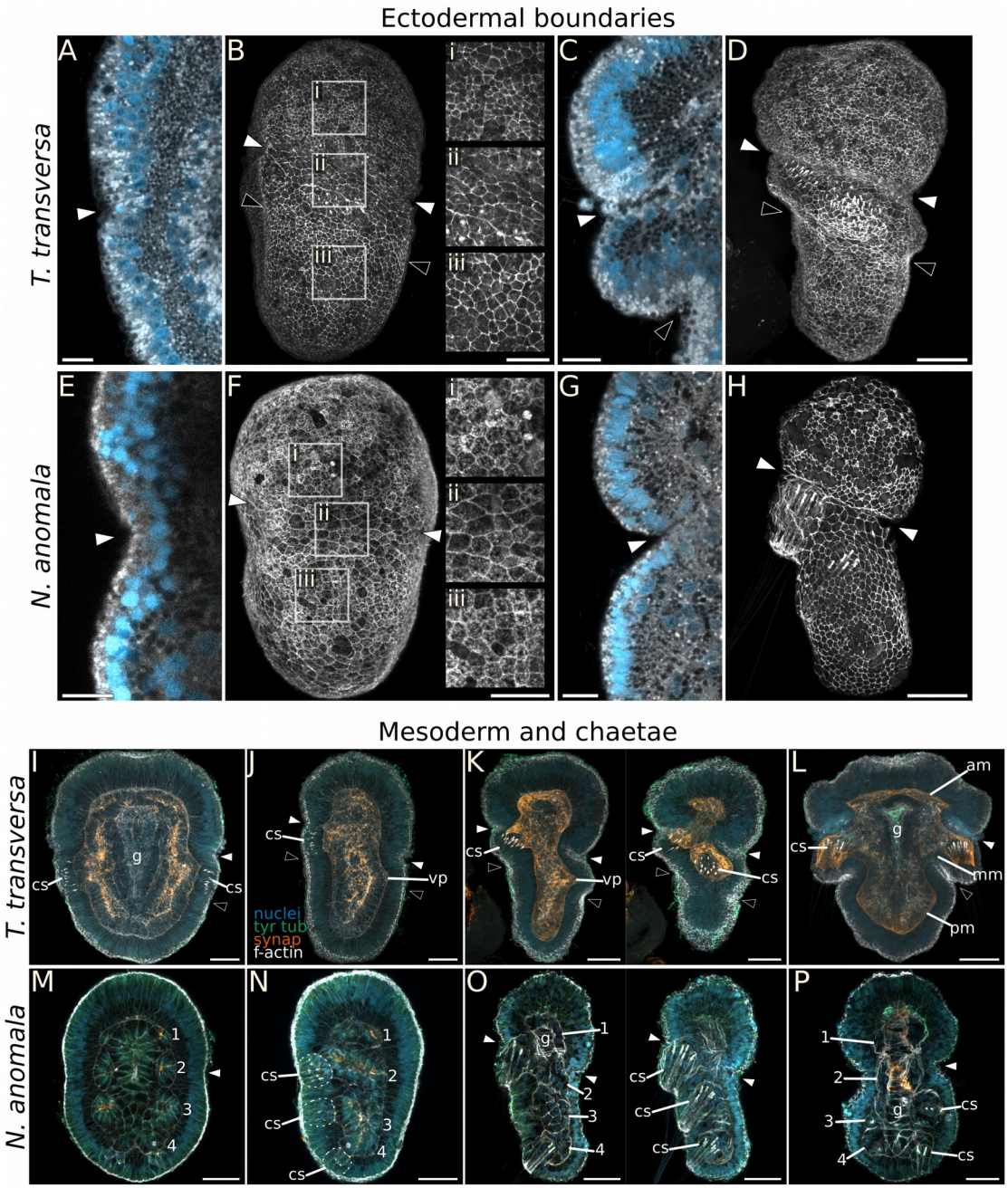

Figure 3. Morphology of the ectodermal and mesodermal boundaries in the larvae of the brachiopods *T. transversa* and *N. anomala*. (A,E) Outline of the apical/mantle furrow in the epidermis of the bilateral gastrula in ventral view. (B,F) Lateral view showing the epidermal surface of the bilateral gastrula showing the membrane outlines of epithelial cells. Boxes mark the regions corresponding to the insets on the right side (i–iii). (C,G) Outline of the apical/mantle furrow in the epidermis of the bilobed larva in ventral view. (D,H) Lateral view showing the epidermal surface of the bilobed larva showing the membrane outlines of epithelial cells. (I,M) Mesoderm morphology at the bilateral gastrula in a ventral view. (J,N) Same stage, but lateral view. (K,O) Bilobed larva showing a more medial (left) and a more lateral (right) slices of and embryo in lateral view. (L,P) Ventral view of a *T. transversa* trilobed larva (L) and a developed bilobed larva of *N. anomala* (P) showing the final arrangement of the larval mesoderm. Nuclei stained with DAPI (blue) and cytoplasmic staining (gray) obtained by mounting specimens stained with BODIPY FL in Thiodiethanol (A,C,E,G). Cell membrane outlines (F-Actin) stained with BODIPY FL mounted in Murray's Clear

bioRxiv preprint doi: https://doi.org/10.1101/029892; this version posted January 25, 2016. The copyright holder for this preprint (which was not certified by peer review) is the author/funder, who has granted bioRxiv a license to display the preprint in perpetuity. It is made available under aCC-BY 4.0 International license.

(B,D,F,H). Mesoderm evidenced by the antibody Anti-Synapsin II (vermillion) with the counter staining of tyrosinated tubulin (green), F-Actin (white) and DAPI (blue) (I–P). Anti-Synapsin II cross-react with an unknown component of *T. transversa* mesoderm and was used as a marker; this reaction is weaker and less specific in *N. anomala*. The four coelomic sacs of *N. anomala* are indicated by numerals 1-4 from anterior to posterior. cs: chaetae sac, g: gut, vp: ventral projection, am: apical mesoderm, mm: mantle mesoderm, pm: pedicle mesoderm. White arrowheads mark the apical/mantle boundary and black arrowheads mark the mantle/pedicle boundary. Anterior is top and ventral is to the right in lateral views for all panels. Scale bars = 20 µm (B,D,F,H,I–P), 10 µm (A,C,E,G).

bioRxiv preprint doi: https://doi.org/10.1101/029892; this version posted January 25, 2016. The copyright holder for this preprint (which was not certified by peer review) is the author/funder, who has granted bioRxiv a license to display the preprint in perpetuity. It is made available under aCC-BY 4.0 International license.

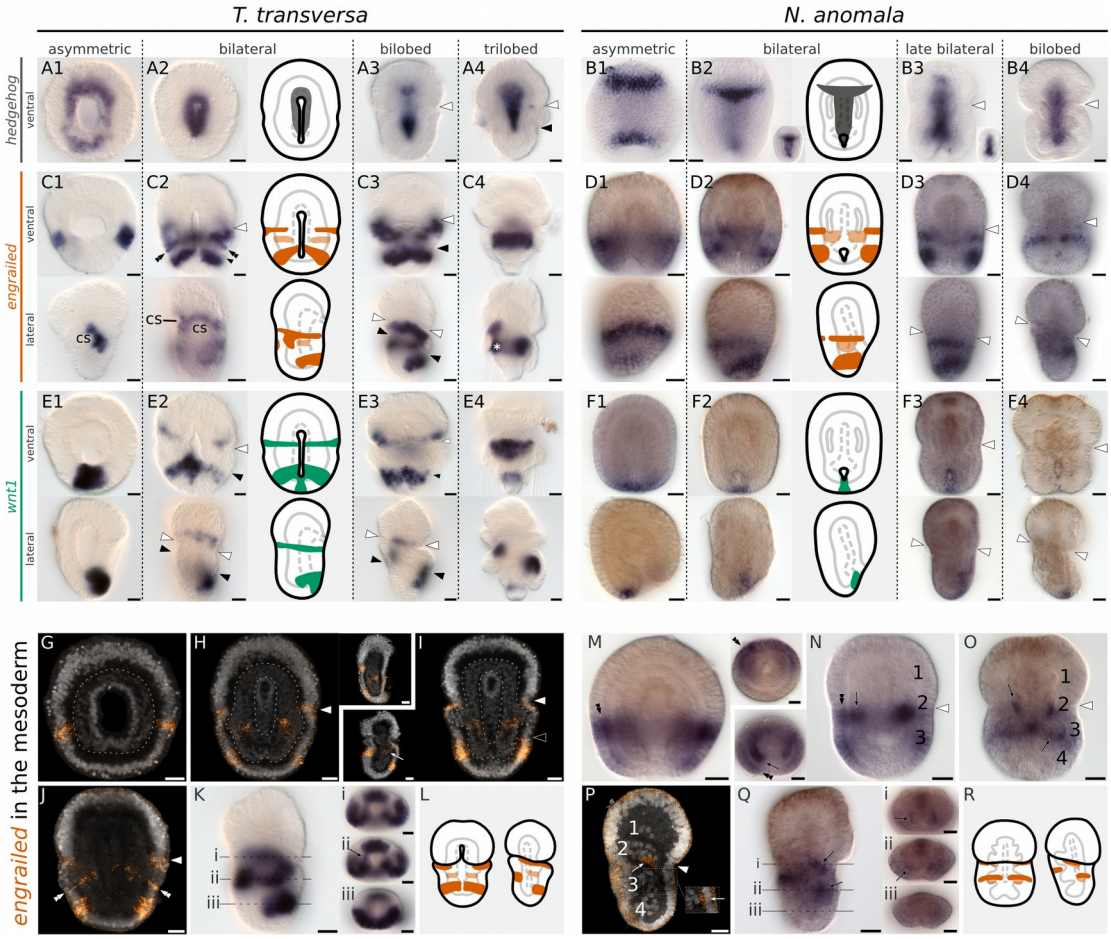

Figure 4. Whole mount in situ hybridization of *hh*, *en* and *wnt1* orthologs in representative developmental stages of the brachiopods *T. transversa* and *N. anomala*. Anterior is top in all panels and ventral is to the right in all lateral views. (A–B) Expression of *hh*. (C–D) Expression of *en*. (E–F) Expression of *wnt1*. Line drawings represent expression at the bilateral gastrula stage. (G–L) Expression of *en* in the mesoderm of *T. transversa*. White dashed lines are highlighting the mesoderm. (G) Asymmetric gastrula with no mesodermal expression of *en*. (H) Onset of mesodermal *en* in the bilateral gastrula in a ventral and lateral view (inset). Specimens are the same of Figure 1C. (I) Resolved bands of *en* in the mesoderm of the bilobed larva in a ventral and lateral view (inset). (J) Connection between ectoderm and mesoderm expression of *en* in a bilateral gastrula. (K) Lateral view of bilobed larva. Black dashed lines mark the position of the optical sections of a posterior view of the same embryo (insets i–iii). (L) Line drawings represent expression at the bilobed stage of *T. transversa*. (M–R) Expression of *en* in the mesoderm of *N. anomala*. (M) Asymmetric gastrula with no mesodermal staining of *en* in a ventral and posterior view (inset). (N) Strong *en* domains in the mesoderm of the bilateral gastrula adjacent to the ectodermal domains at the posterior region of coelomic sac "2". Inset shows the mesoderm in a posterior view. (O) Two pairs of mesodermal domains of *en* in the coeloms "2" and "3" of the bilobed larva. (P) Detail of *en* expression in the bilobed larva in the coeloms "2" and "3" (inset). (Q) Lateral view and optical sections of a posterior view of a bilobed larva showing the expression in the coelomic sacs (insets). (R) Line drawings represent expression at the bilobed stage of *N. anomala*. White arrowheads mark the apical/mantle boundary and black arrowheads mark the mantle/pedicle boundary. Double arrowheads mark the ectodermal expression of *en* while arrows point to the

bioRxiv preprint doi: https://doi.org/10.1101/029892; this version posted January 25, 2016. The copyright holder for this preprint (which was not certified by peer review) is the author/funder, who has granted bioRxiv a license to display the preprint in perpetuity. It is made available under aCC-BY 4.0 International license.

mesodermal domains. Asterisk marks area of unspecific staining due to the rudiment of larval shell (C4). The four coelomic sacs of *N. anomala* are indicated by numerals 1-4 from anterior to posterior. cs: chaetae sacs. Scale bars = 20 µm.

bioRxiv preprint doi: https://doi.org/10.1101/029892; this version posted January 25, 2016. The copyright holder for this preprint (which was not certified by peer review) is the author/funder, who has granted bioRxiv a license to display the preprint in perpetuity. It is made available under aCC-BY 4.0 International license.

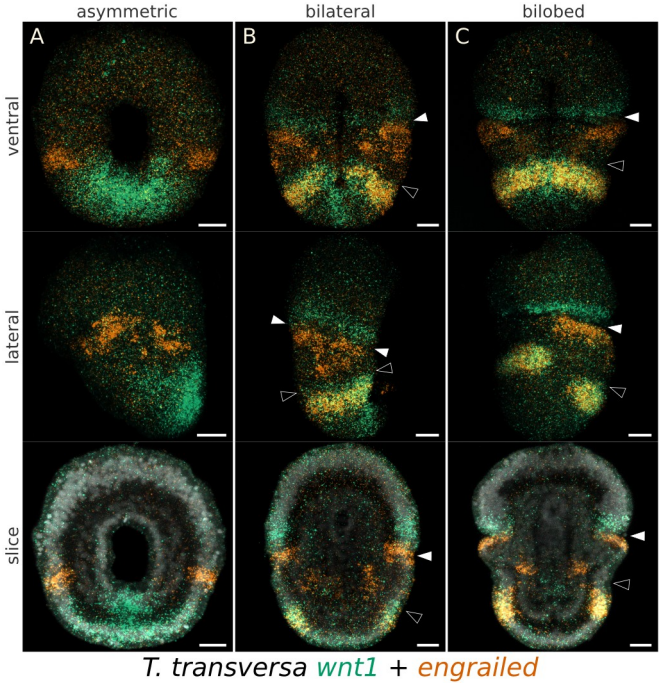

Figure 5. Whole mount double fluorescent in situ hybridization with *en* (vermillion) and *wnt1* (green) in *T. transversa*. (A) Asymmetric gastrula. Same specimens of Figure 1B. (B) Bilateral gastrula. Same specimens of Figure 1C. (C) Bilobed larva. Ventral view is the same specimen of Figure 1D. Ventral and lateral views are maximum intensity projections. Slice view shows additional counter staining with DAPI (gray). Merge (yellow) shows the coexpression of *en* and *wnt1*. Scale bars = 20 µm.

bioRxiv preprint doi: https://doi.org/10.1101/029892; this version posted January 25, 2016. The copyright holder for this preprint (which was not certified by peer review) is the author/funder, who has granted bioRxiv a license to display the preprint in perpetuity. It is made available under aCC-BY 4.0 International license.

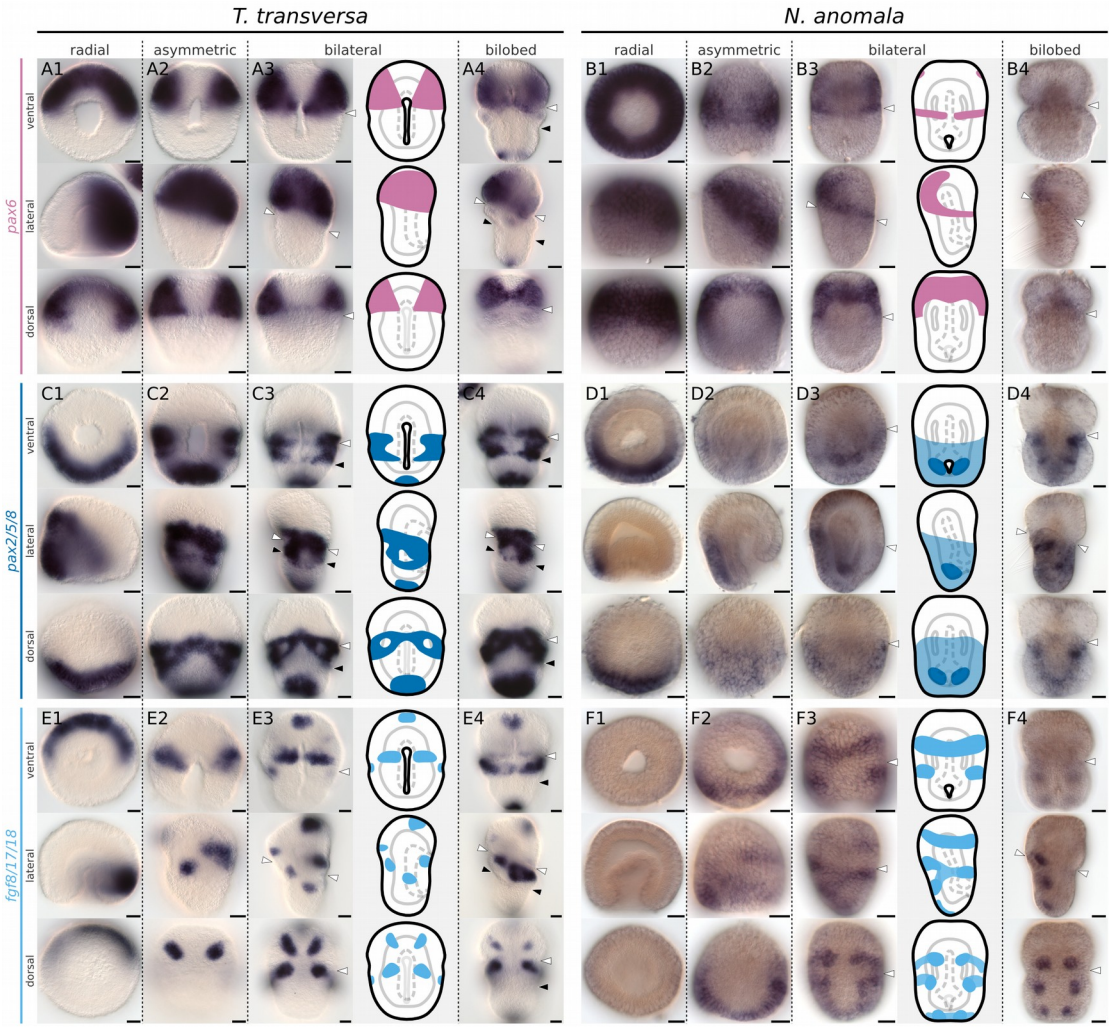

Figure 6. Whole mount in situ hybridization of *pax6*, *pax2/5/8* and *fgf8/17/18* orthologs in representative developmental stages of the brachiopods *T. transversa* and *N. anomala*. (A–B) Expression of *pax6*. (C–D) Expression of *pax2/5/8*. (E–F) Expression of *fgf8/17/18*. Anterior is top in all panels and ventral is to the right in all lateral views. Line drawings represent expression at the bilateral gastrula stage. White arrowheads mark the apical/mantle boundary and black arrowheads mark the mantle/pedicle boundary. Scale bars = 20 µm.

bioRxiv preprint doi: https://doi.org/10.1101/029892; this version posted January 25, 2016. The copyright holder for this preprint (which was not certified by peer review) is the author/funder, who has granted bioRxiv a license to display the preprint in perpetuity. It is made available under aCC-BY 4.0 International license.

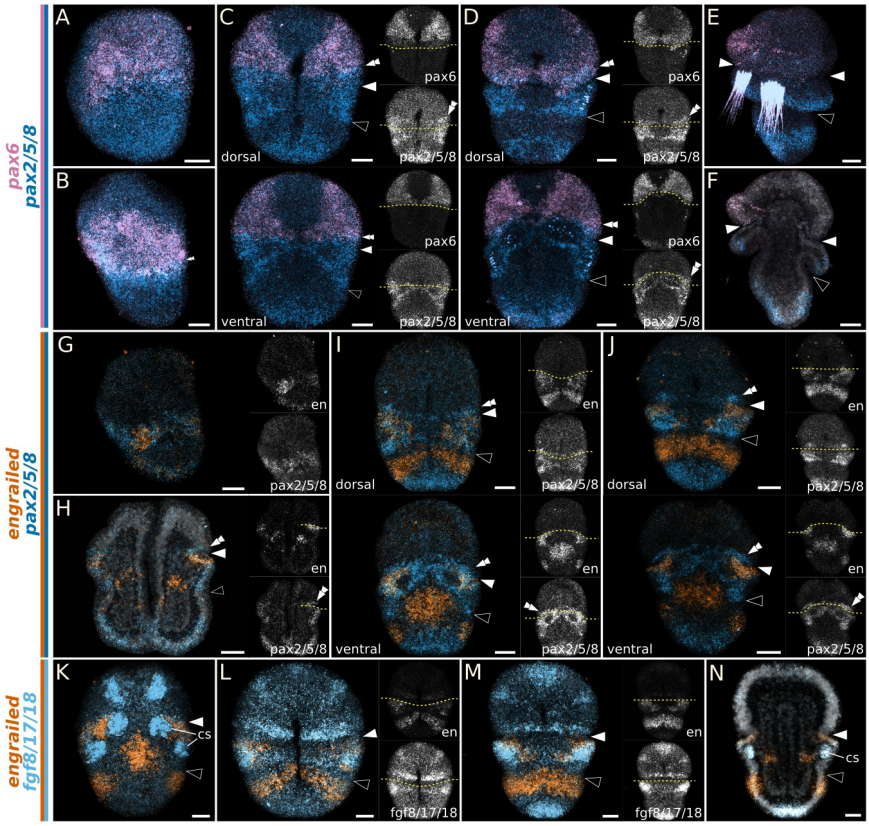

Figure 7. Whole mount double fluorescent in situ hybridization of *pax6* + *pax2/5/8* (A–F), *en* + *pax2/5/8* (G–J) and *en* + *fgf8/17/18* (K–N) in the brachiopod *T. transversa*. (A) Radial gastrula. (B,G) Asymmetric gastrula. (C,H,I,K,L) Bilateral gastrula. (D,J,M,N) Bilobed larva. (E,F) Trilobed larva. Anterior is top in all panels and ventral is to the right in all lateral views. Side panels show the relation between gene expression and the apical/mantle boundary (striped yellow line). White arrowheads mark the apical/mantle boundary and black arrowheads mark the mantle/pedicle boundary. Scale bars = 20 µm.

bioRxiv preprint doi: https://doi.org/10.1101/029892; this version posted January 25, 2016. The copyright holder for this preprint (which was not certified by peer review) is the author/funder, who has granted bioRxiv a license to display the preprint in perpetuity. It is made available under aCC-BY 4.0 International license.

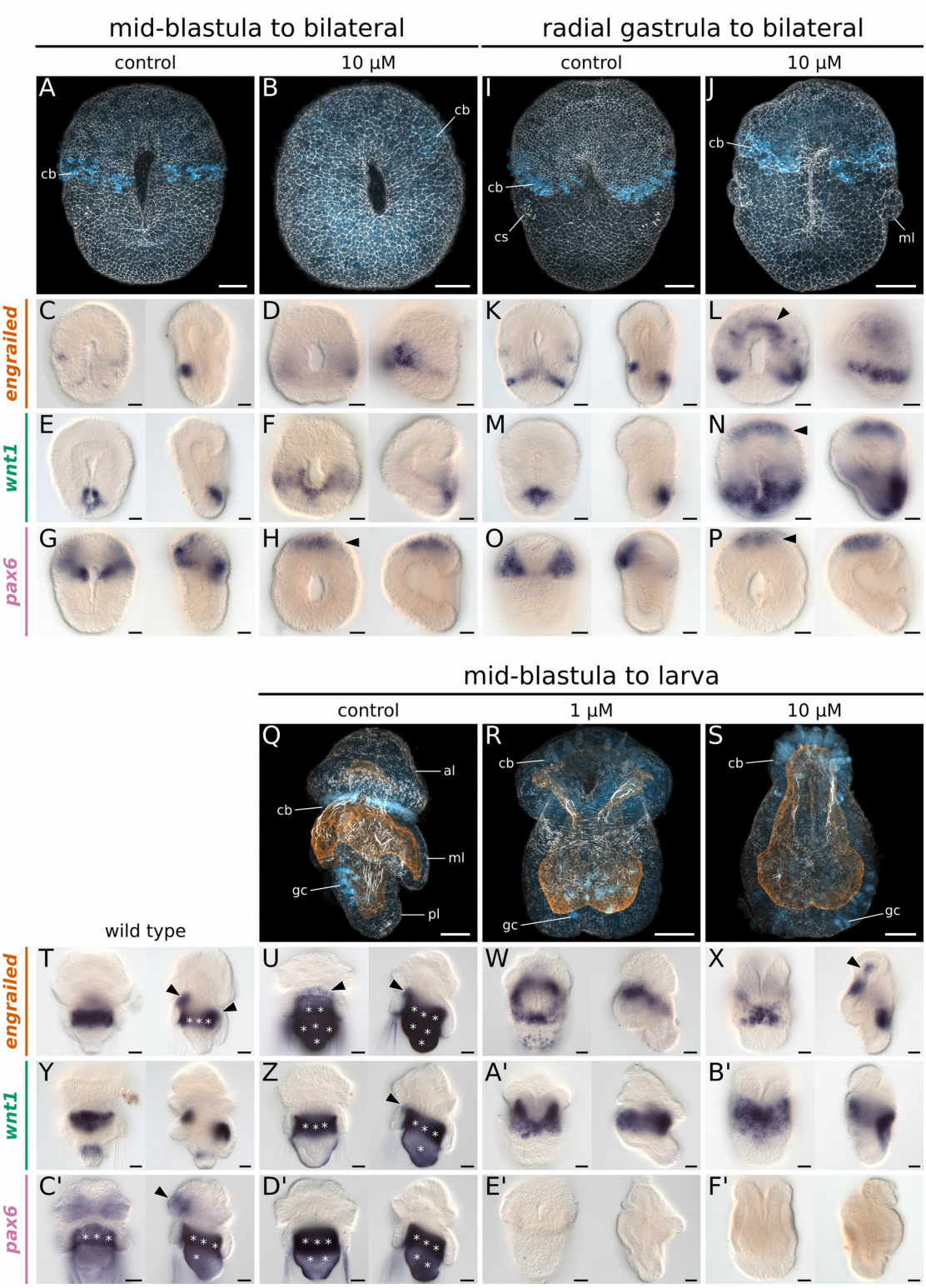

Figure 8. Effects of the over-activation of the canonical Wnt pathway on the morphology and gene expression during the embryonic development of *T. transversa*. We treated developing embryos of *T. transversa* with 1 and 10 µM 1-azakenpaullone diluted in seawater with the following incubation periods: mid-blastula to bilateral gastrula stage (A–H), radial gastrula to bilateral gastrula stage (I–P) and mid-blastula to trilobed larval stage (Q–F'). (A, B) Control and treated samples from mid-blastula to bilateral gastrula. Embryos did not elongate and the disposition of corpuscular bodies (cb)—cells of unknown function that protrude out of the epithelium—is disrupted. (I, J) Control and treated samples from radial gastrula to bilateral gastrula. Embryos

bioRxiv preprint doi: https://doi.org/10.1101/029892; this version posted January 25, 2016. The copyright holder for this preprint (which was not certified by peer review) is the author/funder, who has granted bioRxiv a license to display the preprint in perpetuity. It is made available under aCC-BY 4.0 International license.

do not have a well defined apical/mantle furrow and show bilateral stubs correspondent to incipient mantle lobe tissue. Treated embryos show no sign of chaetae formation. (C–L) Expression of *en* in control and treated embryos. Control embryos have an apical/mantle stripe, a ventral and a dorsal domain of *en*. Early (mid-blastula) and late (radial gastrula) treatments show a posterior laterodorsal *en* domain, but only in the latter we detected an anterior *en* domain consisting of scattered ectodermal cells and a broad mesodermal domain in the anterior end (arrowhead). (E–N) Expression of *wnt1* in control and treated embryos. Control embryos have *wnt1* expressed around the posterior lip of the blastopore. In the treated samples there is an expansion of this posterior domain, occupying half of the blastopore length. Only embryos treated at the radial gastrula stage show an anterior expression domain of *wnt1* at the apical plate (arrowhead), separated from the posterior domain by a subterminal band clear of expression. (G–P) Expression of *pax6* in control and treated embryos. Control embryos have *pax6* transcripts contained in the apical lobe. In all treated embryos the expression of *pax6* shifts anteriorly localizing to the apical plate (arrowheads). (Q–S) Control and treated samples from mid-blastula to larva. (Q) Morphology of control larvae incubated with DMSO is consistent with a wild type trilobed larva of *T. transversa*. The apical lobe has a row of corpuscular bodies at its posterior portion just above the apical/mantle furrow. The mantle lobe has outgrown with the extensive underlying mesoderm and musculature, and the pedicle lobe shows dorsal putative gland cells (gc). (R–S) Morphology of treated embryos developed into larvae reveals an expansion of posterior structures. Larval body has a distinct anterior portion covered by corpuscular bodies and an unclosed blastoporal opening at its center (R). Higher concentrations of 1-azakenpaullone (10 µM) resulted in a diminished anterior portion (S). Morphology of the posterior portion resembles an over-developed pedicle lobe with putative gland cells on the dorsal side. The anterior and posterior regions of treated embryos are demarcated by an ectodermal fold. We neither detected signs of chaetae sacs nor evidence for the presence of a mantle lobe. (T–X) Expression of *en* in wild type, control and treated embryos. Wild type expression of *en* consists of a ventral and a dorsal domain in the pedicle lobe (T, arrowheads; same specimen as Figure 4C4). Control embryos have a similar pattern, although regions of unspecific staining in the pedicle lobe (*) obfuscate the signal (U, arrowhead). Treated embryos show a broader expression domain of *en* encircling the embryo at the anterior portion of the pedicle lobe, similar to wild type and controls (W, X). At 10 µM, *en* is also expressed in the mesoderm at the anterior end (X, arrowhead). (Y–B') Expression of *wnt1* in wild type, control and treated embryos. Wild type expression of *wnt1* colocalizes with *en* expression (T), except for an additional posterior domain at the pedicle lobe (Y, same specimen as Figure 4E4). Control embryos also display shell background (*), but signal at the dorsal side is visible (Z, arrowhead). Transcripts of *wnt1* in treated embryos occupy the same territories as *en* (W, X), except for the absence of *wnt1* in the anterior mesoderm (B'). (C'–F') Expression of *pax6* in wild type, control and treated embryos. Wild type expression of *pax6* occurs in the dorsal portion of the apical lobe (arrowhead). We did not detect transcripts of *pax6* in control (D') or treated embryos (E', F'). Scores represent the number of embryos with the phenotype shown in the panel against the total number of embryos analyzed: (C) 34/48, (D) 36/41, (E) 25/26, (F) 27/33, (G) 25/26, (H) 13/18, (K) 28/36, (L) 58/88 (21/88 without anterior mesodermal domain), (M) 56/59, (N) 57/72 (12/72 without anterior domain), (O) 28/31, (P) 51/53, (U) 30/33, (W) 38/43, (X) 47/66 (11/66 without anterior mesodermal domain), (Z) 13/24, (A') 34/38, (B') 37/41, (D') 24/24, (E') 36/36, (F') 29/29. Asterisks (*) mark unspecific staining due to the secretion of the larval shell in *T.*

bioRxiv preprint doi: https://doi.org/10.1101/029892; this version posted January 25, 2016. The copyright holder for this preprint (which was not certified by peer review) is the author/funder, who has granted bioRxiv a license to display the preprint in perpetuity. It is made available under aCC-BY 4.0 International license.

transversa. cb: corpuscular bodies, gc: putative gland cells, al: apical lobe, ml: mantle lobe, pl: pedicle lobe, cs: chaetae sacs. Scale bars = 20 µm.

bioRxiv preprint doi: https://doi.org/10.1101/029892; this version posted January 25, 2016. The copyright holder for this preprint (which was not certified by peer review) is the author/funder, who has granted bioRxiv a license to display the preprint in perpetuity. It is made available under aCC-BY 4.0 International license.

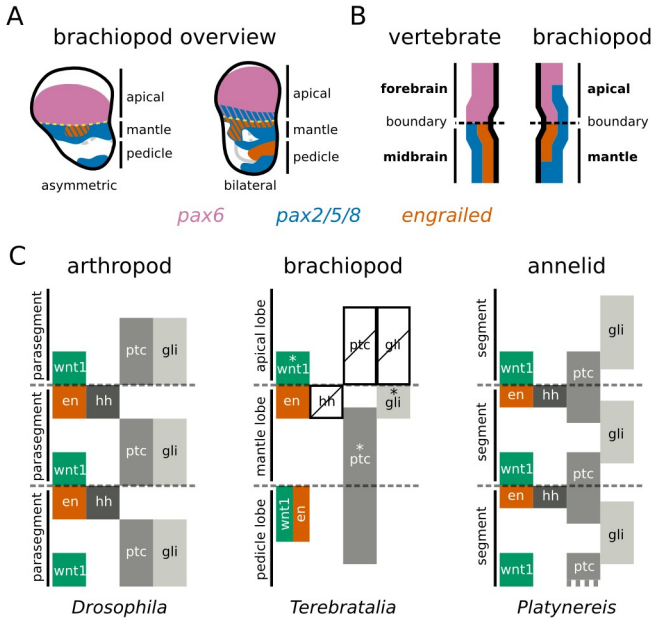

Figure 9. Summary of brachiopod gene expression and comparison to other organisms. (A) Expression of genes related to the apical/mantle boundary with consistent expression between the brachiopods *T. transversa* and *N. anomala* (*pax6*, *pax2/5/8* and *en*). (B) Spatial relationship between the expression of *pax6*, *pax2/5/8* and *en* in the di/mesencephalon boundary of the vertebrate brain and the apical/mantle boundary in the brachiopod larval body. (C) Expression patterns of the segment polarity genes *en*, *wnt1*, *hh*, *ptc* and *gli* in relation to the parasegments of an arthropod (*D. melanogaster*), larval lobes of a brachiopod (*T. transversa*) and the trunk segments of an annelid (*P. dumerilii*). White boxes with black border indicate the expected localization of transcripts for a segment polarity role which are absent in *T. transversa*. Asterisks mark expression patterns that are variable between *T. transversa* and *N. anomala*.

bioRxiv preprint doi: https://doi.org/10.1101/029892; this version posted January 25, 2016. The copyright holder for this preprint (which was not certified by peer review) is the author/funder, who has granted bioRxiv a license to display the preprint in perpetuity. It is made available under aCC-BY 4.0 International license.

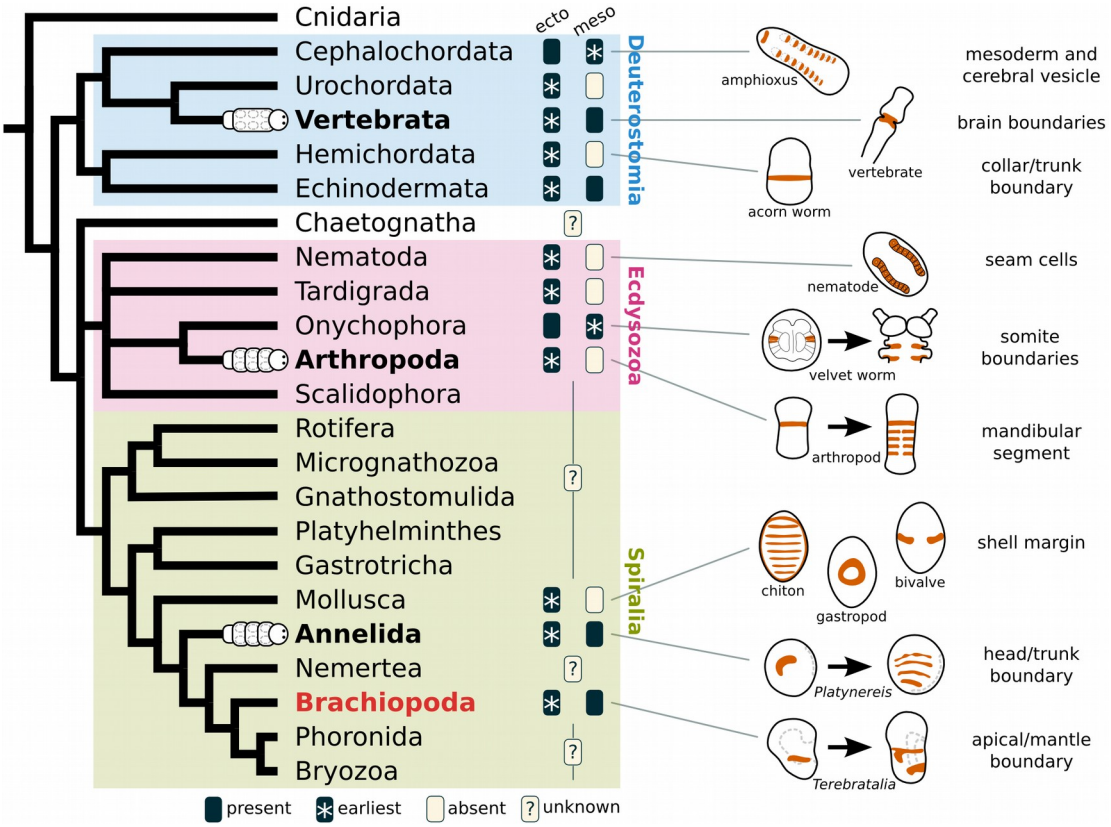

Figure 10. Comparative *en* expression in bilaterians. Phylogenetic tree based on (Laumer *et al.* 2015) and data compiled on Table S1. Dark boxes indicate *en* is expressed in the ectoderm (left column) and mesoderm (right column). Boxes with asterisk indicate the tissue where *en* is first expressed (ectoderm or mesoderm). Light boxes mark when *en* is not found in the ectoderm or mesoderm. Drawings show expression of *en* (vermillion) in embryonic stages of representative groups. Structures associated with *en* expression in each group are listed on the right.

bioRxiv preprint doi: https://doi.org/10.1101/029892; this version posted January 25, 2016. The copyright holder for this preprint (which was not certified by peer review) is the author/funder, who has granted bioRxiv a license to display the preprint in perpetuity. It is made available under aCC-BY 4.0 International license.

Additional files

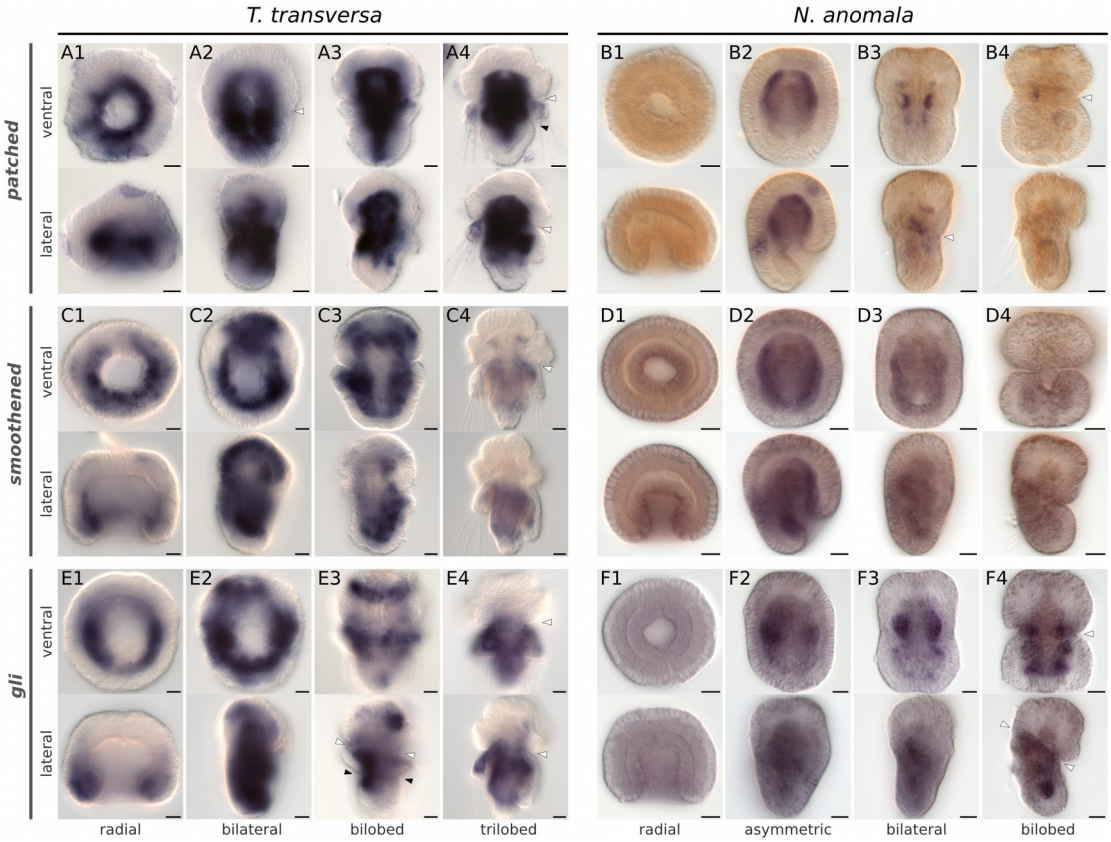

Additional file 1: Figure S1. Whole mount in situ hybridization of the Hedgehog pathway orthologs in representative developmental stages of the brachiopods *T. transversa* and *N. anomala*. (A,B) Expression of *T. transversa ptc* and *N. anomala ptc1*. (C,D) Expression of *smo*. (E,F) Expression of *gli*. In the radial gastrula, transcripts of *ptc*, *smo* and *gli* occur in the mesoderm of *T. transversa* (A1,C1,E1). Transcripts of *ptc* are expressed in the mesoderm and endoderm of *T. transversa* of subsequent stages (A2–A4), except at the posterior pedicle mesoderm (A3,A4). *N. anomala ptc1* is not expressed in the radial gastrula (B1). Expression is restricted to the anterior mesoderm of the asymmetric gastrula (B2); dorsal and anterior ectodermal spots are also present at this stage. Transcripts of *ptc1* remain in the ventral mesoderm associated with the first, second and third coelomic sacs (B3) and fade in the bilobed larva of *N. anomala* (B4). *T. transversa smo* is ubiquitously expressed in the mesoderm during gastrulation (C1–C3). In the asymmetric and bilateral gastrula we observed a conspicuous anterior *smo* ectodermal domain as well as expression on the dorsal side (C2,C3). Expression was cleared from the anterior mesoderm in the trilobed larva (C4). We first detected the expression of *N. anomala smo* in the asymmetric gastrula covering most of the mesoderm except for the anterior portion correspondent to the first coelomic sac (D2); a dorsal ectodermal domain is also present. The expression fades in the bilateral gastrula and *smo* is not detected in the bilobed larva (D3,D4). *T. transversa gli* is expressed in the whole mesoderm of the radial and asymmetric gastrula (E1,E2) and in two ectodermal domains, anterior region of the apical lobe and mantle lobe (E2). Expression becomes restricted to patches in the mantle mesoderm and the ectodermal domains resolve into stripes in the anterior portion of the apical and mantle lobes (E3). Finally, in the trilobed larva transcripts of *gli* are restricted to the mantle and pedicle mesoderm (E4). *N. anomala gli* is expressed in the forming second to fourth coelomic pouches but not the in the first (F2–F4) and the expression

bioRxiv preprint doi: https://doi.org/10.1101/029892; this version posted January 25, 2016. The copyright holder for this preprint (which was not certified by peer review) is the author/funder, who has granted bioRxiv a license to display the preprint in perpetuity. It is made available under aCC-BY 4.0 International license.

covers most of the mesoderm in the bilobed larva (F4). Overall, the expression of the Hedgehog pathway components are localized to the endoderm and mesoderm and do not correlate with the development of ectodermal boundaries in both brachiopod species. Anterior is top in all panels and ventral is to the right in all lateral views. White arrowheads mark the apical/mantle boundary and black arrowheads mark the mantle/pedicle boundary. Scale bars = 20 µm.

bioRxiv preprint doi: https://doi.org/10.1101/029892; this version posted January 25, 2016. The copyright holder for this preprint (which was not certified by peer review) is the author/funder, who has granted bioRxiv a license to display the preprint in perpetuity. It is made available under aCC-BY 4.0 International license.

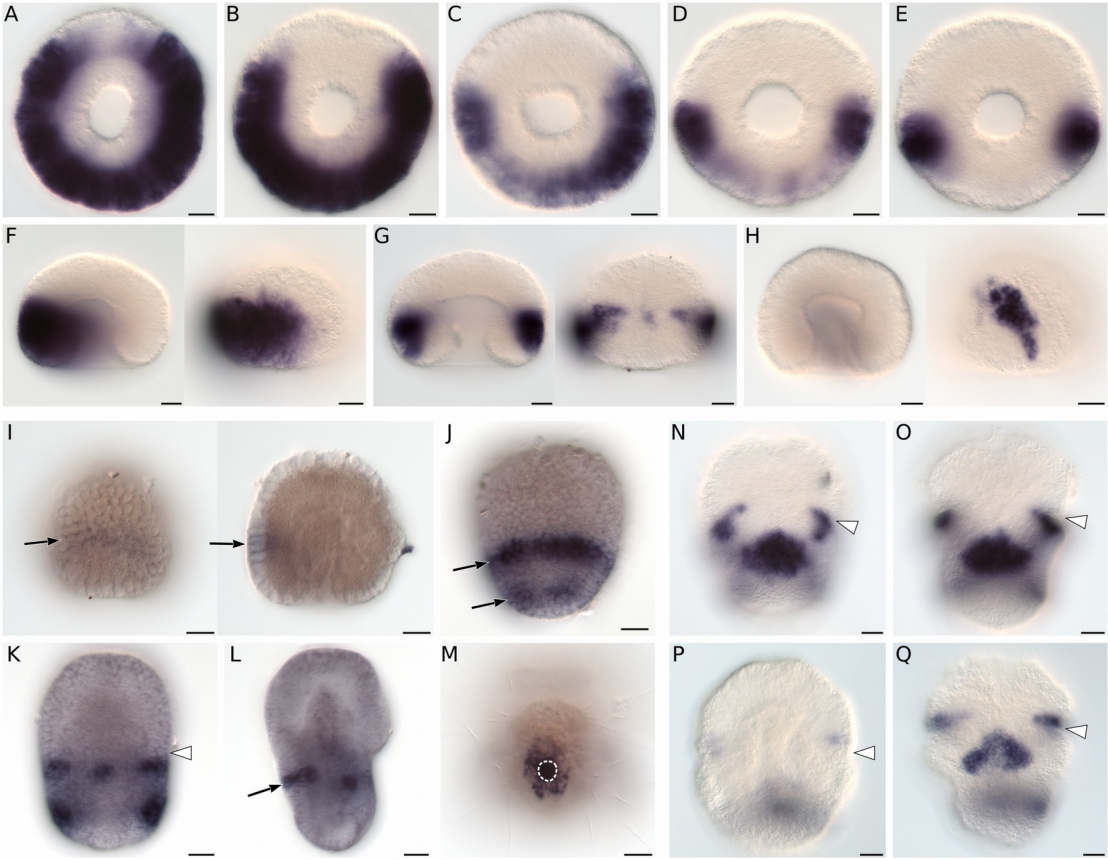

Additional file 2: Figure S2. Additional details about the embryonic expression of *en* and *wnt1* in the brachiopods *T. transversa* and *N. anomala*. (A–E) Dynamic progression of *en* transcripts at the radial gastrula of *T. transversa* in blastoporal view. (F,G,H) Lateral views correspondent to (B,D,E), respectively, with anterior to the right side. (I) Dorsal (left) and lateral view (right) of *N. anomala* radial gastrula showing faint *en* stripe (arrow). (J) Dorsal view of *N. anomala* asymmetric gastrula with two stripes of *en* (arrows). (K) Dorsal view of *N. anomala* bilateral gastrula. (L) Conspicuous dorsal domain of *en* associated with the shell rudiment in the bilobed larva of *N. anomala* in lateral view (arrow). (M) Developed larva of *N. anomala* with shell primordium. Original area with *en* signal is outlined by white dashed line. Surrounding area is likely unspecific staining related to the shell deposition. (N) Dorsal view of a *T. transversa* bilateral larva showing *en* expression. (O) Same view as (N) showing *en* expression at the subsequent bilobed larva stage. (P) Absence of *wnt1* expression on the dorsal side of *T. transversa* bilateral gastrula. (Q) Same view as (P) showing dorsal *wnt1* domain of *T. transversa* bilobed larva. Scale bars = 20 µm.

bioRxiv preprint doi: https://doi.org/10.1101/029892; this version posted January 25, 2016. The copyright holder for this preprint (which was not certified by peer review) is the author/funder, who has granted bioRxiv a license to display the preprint in perpetuity. It is made available under aCC-BY 4.0 International license.

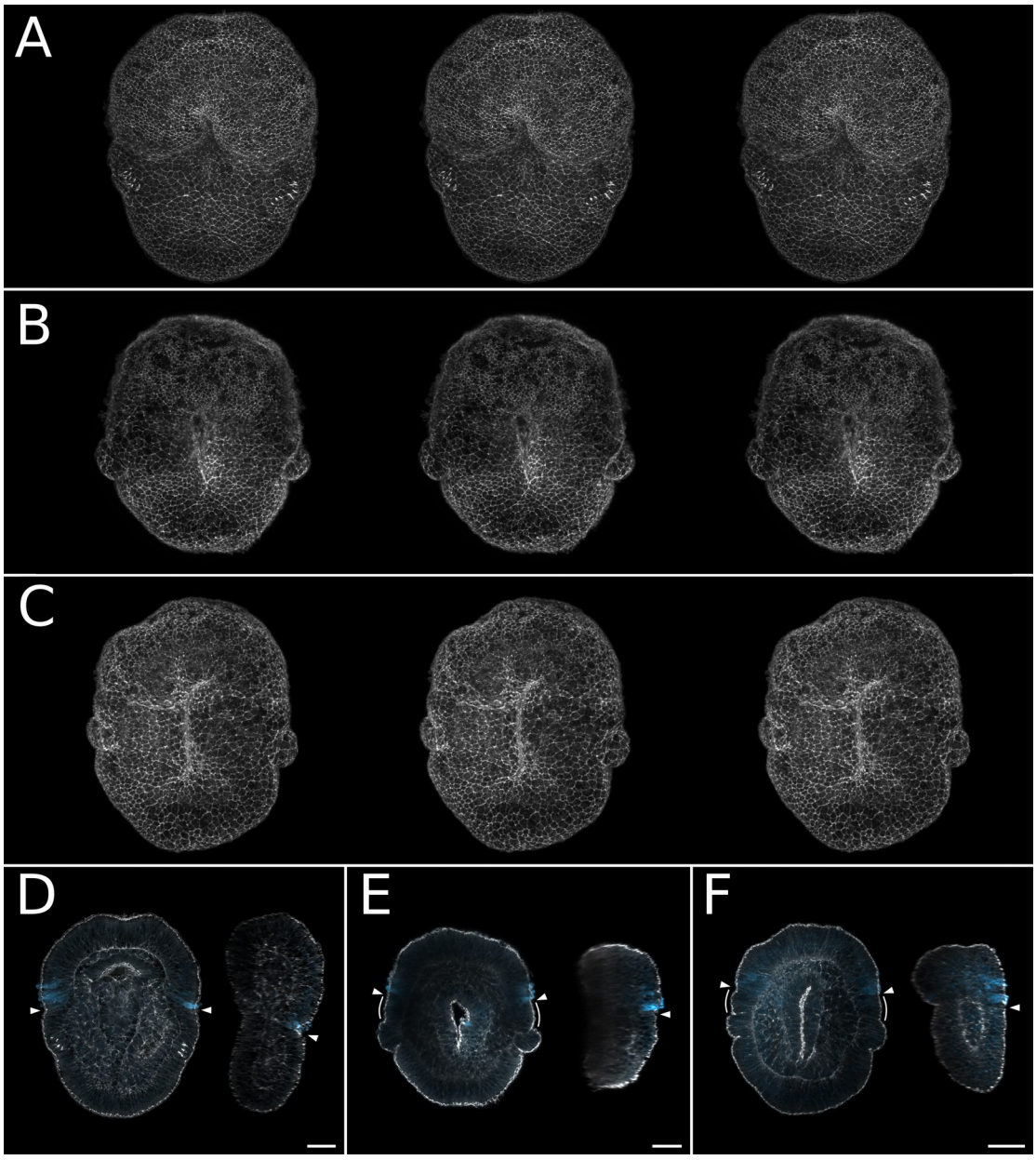

Additional file 3: Figure S3. Perturbation of the apical/mantle boundary during over-activation of Wnt pathway in *T. transversa*. We treated developing embryos of *T. transversa* from radial gastrula to bilateral gastrula stage with 1 µM and 10 µM 1-aza-kenpaullone diluted in seawater. (A–C) Stereo images showing a maximum intensity projection of the epithelial surface of embryos stained for F-actin (cell membranes in white). (D–F) Maximum intensity projections of five inner slices (left) and orthogonal views (right) of the same embryos as above, but including a nuclei staining (blue) to highlight the position of corpuscular bodies. Control sample incubated with DMSO show the characteristic ectodermal furrow at the apical/mantle boundary (A, D). Embryos treated with 1 µM (B, E) and 10 µM (C, F) 1-azakenpaullone do not form a furrow at the apical/mantle boundary. Embryos treated with 1 µM (E) and 10 µM (F) 1-azakenpaullone do not form a. Absence of an ectodermal furrow at the apical/mantle boundary (arrowheads). White line marks the area between the expected furrow position and the mantle lobe stub in treated embryos (E, F). Scale bars = 20 µm.

Additional file 4: Table S1. Summary of embryonic expression of *en*, *pax6* and *pax2/5/8* across bilaterians. Dashes represent absence of expression and question marks represent missing data. Expression information based on Cephalochordata *en* (Holland *et al.* 1997), *pax6* (Glardon *et al.* 1998) and *pax2/5/8* (Kozmik *et al.* 1999); Urochordata *en* (Cañestro *et al.* 2005; Imai *et al.* 2002; Jiang & Smith 2002), *pax6* (Glardon *et al.* 1997) and *pax2/5/8* (Bassham *et al.* 2008; Cañestro *et al.* 2005; Wada *et al.* 1998); Vertebrata *en* (Brivanlou & Harland 1989; Danielian & McMahon 1996; Davis *et al.* 1991; Ekker *et al.* 1992; Hatta *et al.* 1991; Holland *et al.* 1993; Joyner 1996; Njølstad & Fjose 1988; Patel *et al.* 1989), *pax6* (Derobert *et al.* 2002; Püschel *et al.* 1992; Walther & Gruss 1991) and *pax2/5/8* (Heller & Brändli 1999; McCauley & Bronner-Fraser 2002; Pfeffer *et al.* 1998); Hemichordata *en*, *pax6* and *pax2/5/8* (Lowe *et al.* 2003; Pani *et al.* 2012); Echinodermata *en* (Byrne *et al.* 2005; Dolecki & Humphreys 1988; Lowe & Wray 1997; Yaguchi *et al.* 2006) and *pax6* (Omori *et al.* 2011); Nematoda *en* (Cassata *et al.* 2005), *pax6* (Chisholm & Horvitz 1995) and *pax2/5/8* (Rajakumar & Chamberlin 2007); Tardigrada *en* (Gabriel & Goldstein 2007); Onychophora *en* (Eriksson *et al.* 2009; Franke & Mayer 2014), *pax6* (Eriksson *et al.* 2013; Franke *et al.* 2015) and *pax2/5/8* (Franke *et al.* 2015); Arthropoda *en* (Ahzhanov & Kaufman 2000; Brown *et al.* 1994; Damen 2002; DiNardo & O'Farrell 1987; Dougan & DiNardo 1992; Farzana & Brown 2008; Fjose *et al.* 1985; Fleig 1990; Kornberg *et al.* 1985; Manzanares *et al.* 1993, 1996; Marie & Bacon 2000; Mellenthin *et al.* 2006; Patel *et al.* 1989; Whitington *et al.* 1991), *pax6* (Quiring *et al.* 1994) and *pax2/5/8* (Czerny *et al.* 1997); Rotifera *pax6* (Boell & Bucher 2008); Platyhelminthes *pax6* (Callaerts *et al.* 1999); Mollusca *en* (Baratte *et al.* 2007; Hohagen *et al.* 2015; Jacobs *et al.* 2000; Moshel *et al.* 1998; Nederbragt *et al.* 2002; Wanninger & Haszprunar 2001), *pax6* (Hartmann *et al.* 2003; Navet *et al.* 2009; Tomarev *et al.* 1997) and *pax2/5/8* (O'Brien & Degnan 2003; Wollesen *et al.* 2015); Annelida *en* (Bely & Wray 2001; Lans *et al.* 1993; Prud'homme *et al.* 2003; Seaver & Kaneshige 2006; Seaver *et al.* 2001; Wedeen & Weisblat 1991), *pax6* (Arendt *et al.* 2002; Denes *et al.* 2007; Quigley *et al.* 2007) and *pax2/5/8* (Denes *et al.* 2007); Nemertea *pax6* (Tarpin *et al.* 1999).

taxon	***en* (ectoderm)**	***en* (mesoderm)**	***pax6***	***pax2/5/8***
Cephalochordata	Bilateral domains in the brain.	Transverse stripes at posterior region of first eight somites.	Anterior third of neural plate.	Bilateral clusters at the neural plate around fifth somite.
Urochordata	Anterior neuroectoderm.	-	Animal hemisphere in two bilaterally arranged domains.	Bilateral pair of neural tube cells (coexpressed or intercalated with en).
Vertebrata	Mid/hindbrain boundary.	Posterior portion of somites after morphology (muscle pioneers).	Anterior domain bordering the di/mesencephalon border and developing eyes.	Mid/hindbrain boundary. Pronephros, otic vesicle, endostyle.
Hemichordata	Transverse stripe anterior to collar/trunk boundary.	-	Anterior domain bordering the collar/trunk boundary, overlap with *en* domain.	Posterior expression (trunk) adjacent to *en*.

Echinodermata	Pair of serotonin positive cells around the mouth. Adult nervous system.	Lining coelomic sacs.	Anterior wall of the archenteron in the late gastrula.	?
Chaetognatha	?	?	?	?
Nematoda	Bilateral row of epidermal cells (seam cells) and anterior neurons.	-	Anterior head cells.	Egg-laying system during organogenesis.
Tardigrada	Transverse stripes corresponding to posterior region of underlying endomesodermal pouches before ectodermal segmentation.	-	?	?
Onychophora	Segmental transverse stripes at posterior region of segment with no precise boundaries.	Pair of domains in presomitic mesoderm before segments, but sequentially after morphology.	Cephalic lobe expression posterior of the protocerebral/ocular segment.	Segmental expression matching nephridial openings.
Arthropoda	Segmental transverse stripes at parasegmental boundary and posterior region of segment before morphology. Posterior of imaginal discs, adult abdominal segments and nervous system.	Transient segmental expression.	Forming brain, eye primordia, ventral nerve cord and lateral sense organs.	Few cells per segment.
Scalidophora	?	?	?	?
Rotifera	?	?	Anterior bilateral patches.	?
Micrognathozoa	?	?	?	?
Gnathostomulida	?	?	?	?
Platyhelminthes	?	?	Eyes.	?
Gastrotricha	?	?	?	?

Mollusca	Delimiting shell compartment.	-	Optic region, brain and arms.	Apical pole during embryogenesis, anterior region of the mantle, sensory systems and cephalopod brain.
Annelida	Variable. Segmental expression mainly associated to neurons but can occur before morphology.	Mesodermal derivatives (nephrostome).	Anterior bilateral patches abutting the prototroch and eyes. Nervous system before segmentation.	Trunk nervous system.
Nemertea	?	?	Anterior dorsolateral patches in regenerating eyes.	?
Brachiopoda	Two lateral pairs with anterior domain bordering the apical/mantle boundary.	Posterior portion of two coelomic sacs.	Broad anterior domain bordering the apical/mantle boundary.	Expressed in the mantle lobe.
Phoronida	?	?	?	?
Bryozoa	?	?	?	?

bioRxiv preprint doi: https://doi.org/10.1101/029892; this version posted January 25, 2016. The copyright holder for this preprint (which was not certified by peer review) is the author/funder, who has granted bioRxiv a license to display the preprint in perpetuity. It is made available under aCC-BY 4.0 International license.

Additional file 5: Table S2. Gene specific primer pairs used for molecular cloning in *T. transversa* (Ttra) and *N. anomala* (Nano), and gene accession numbers in NCBI.

gene	primers	NCBI accession
Ttra en	R1 CCATCAGATGAAGAGCCAGACCATTTCG	KT253953
	R2 AGTTTTGCTCGTTTGTTTTGGAACC	
Ttra fgf8	F CCGATAGCTTTGGAAGCAAG	KT253954
	R CAATGCCAACAATTCAACCA	
Ttra gli	F CCAGTGAAGCATCTCAAGTGTCG	KT253955
	R CGGTTGCGTGCCATACTATTTTG	
Ttra hh	F AGTGGGAGTTCAGATGGACG	KT253956
	R ATGCTCTCACACGGTCTCAA	
Ttra pax6	F1 GGATAGTGGAACTGGCACACAGCGGAG	KT253957
	F2 CGGATGTGTGAGCAAGATCCTCGGGAG	
Ttra pax258	F TTGCCTGGGAAATACGGGAC	KT253958
	R ATCCAGCTGGTTGACTGGTG	
Ttra ptc	F TTACAGCAGTCAAGAAAGTGGTCG	KT253959
	R TGGGGTTGGATGGATGTTAGC	
Ttra smo	F TGGTCACATTCATTGTCCACCTG	KT253960
	R ATCCTCGGTTTCCTCCTTCTCG	
Ttra wnt1	F TAGCACACACAGGCAAGATAGTCC	KT253961
	R GGAGTAGCAAGTGGAAATGGGG	
Nano en	F ATGTACTCACAGGAGGAGCCACTC	KT253962
	R AGTTGCAGAGCCAATCCGTG	
Nano fgf8	F CAACACGGACACTCCAGAAA	KT253963
	R TATACGGGCTGTTGGTGTCA	
Nano gli	F TCAACAAGGCTACAGTCAGC	KT253964
	R TGCCTTTTATCCTCGTGACG	
Nano hh	F ACCTGAGCAGACGACCAGTT	KT253965
	R AAAATCCCCCAGTTCAAACC	
Nano pax6	F GCAACAGAAGTCAACATGCC	KT253966
	R GACAGGCTGATGGATTGAGG	
Nano pax258	F TGGCTGTGTGAGCAAGATACTCG	KT253967
	R CTGTGAGGAGAGGAGGCATTGTAG	
Nano ptc1	F GGACCCATCCAGCTTTTAGG	KT253968
	R ATCCTGTGTCCAGTCAATGC	
Nano smo	F GCATCCTCTGTACGTGAAGC	KT253969
	R CTCGTACCCAGTGGTTTACG	
Nano wnt1	F CGAGGAACTAAGTGGTGGACATTAG	KT253970
	R TTTCCATCAAGCCCCCTTGG	

bioRxiv preprint doi: https://doi.org/10.1101/029892; this version posted January 25, 2016. The copyright holder for this preprint (which was not certified by peer review) is the author/funder, who has granted bioRxiv a license to display the preprint in perpetuity. It is made available under aCC-BY 4.0 International license.

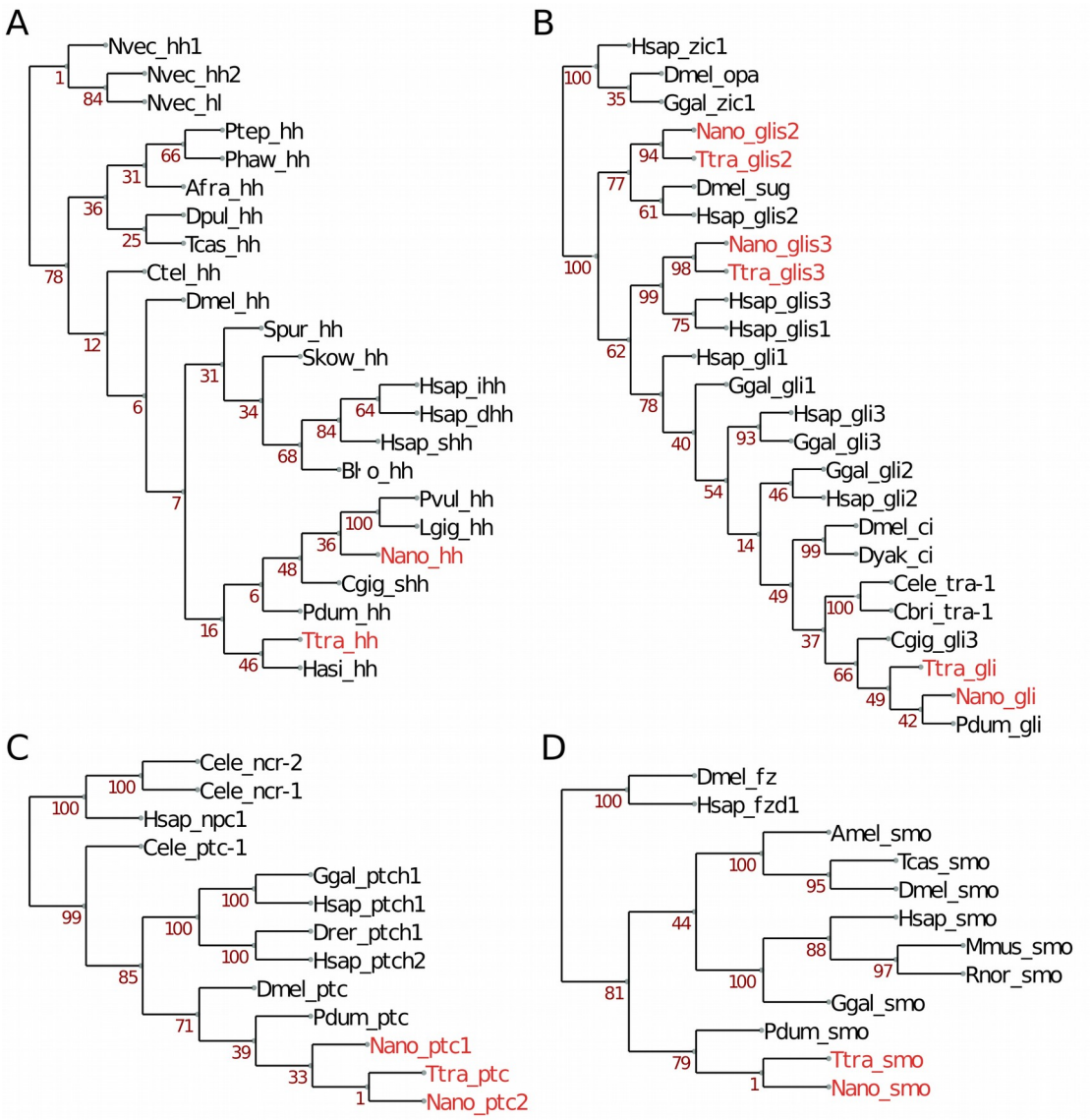

bioRxiv preprint doi: https://doi.org/10.1101/029892; this version posted January 25, 2016. The copyright holder for this preprint (which was not certified by peer review) is the author/funder, who has granted bioRxiv a license to display the preprint in perpetuity. It is made available under aCC-BY 4.0 International license.

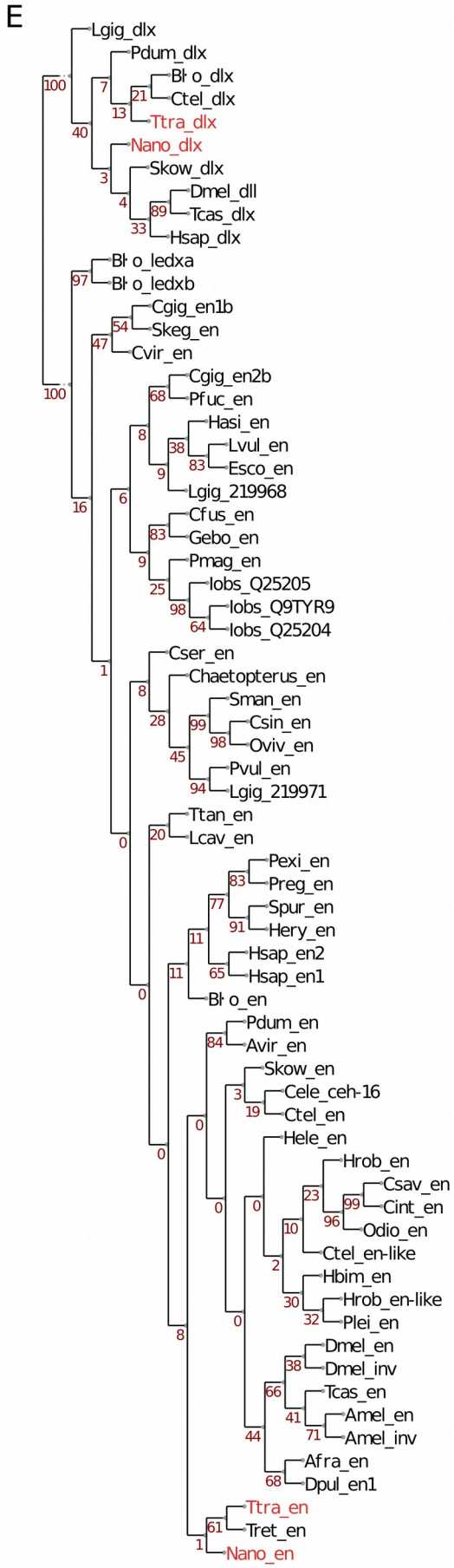

bioRxiv preprint doi: https://doi.org/10.1101/029892; this version posted January 25, 2016. The copyright holder for this preprint (which was not certified by peer review) is the author/funder, who has granted bioRxiv a license to display the preprint in perpetuity. It is made available under aCC-BY 4.0 International license.

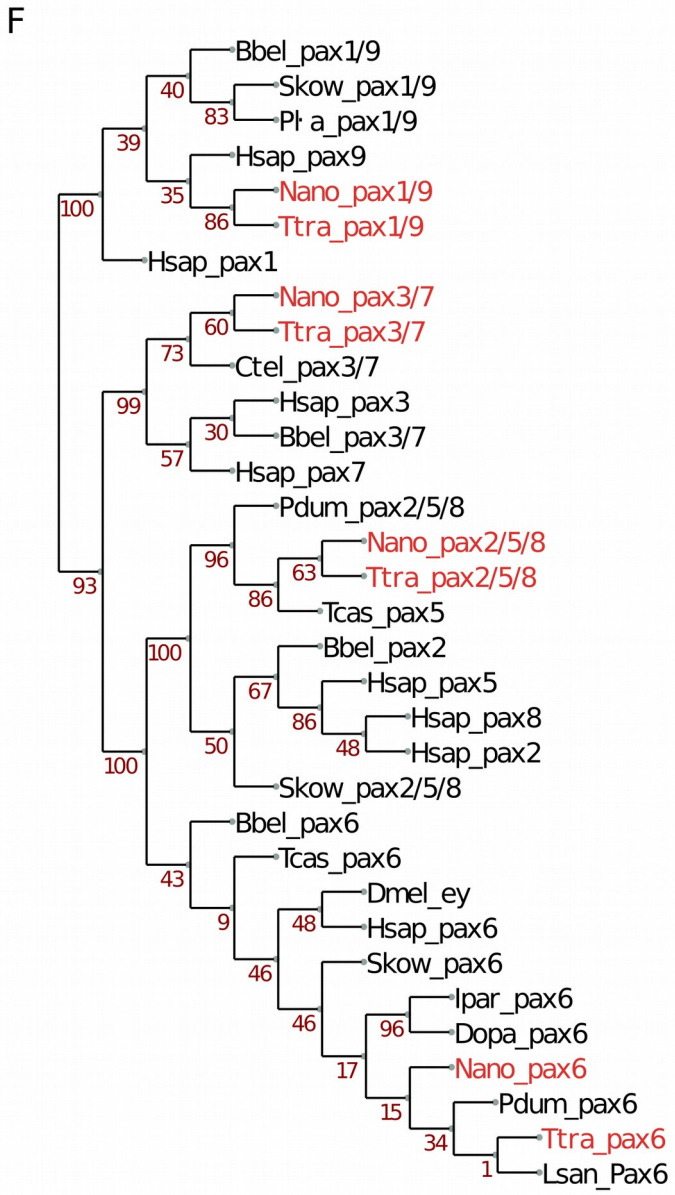

bioRxiv preprint doi: https://doi.org/10.1101/029892; this version posted January 25, 2016. The copyright holder for this preprint (which was not certified by peer review) is the author/funder, who has granted bioRxiv a license to display the preprint in perpetuity. It is made available under aCC-BY 4.0 International license.

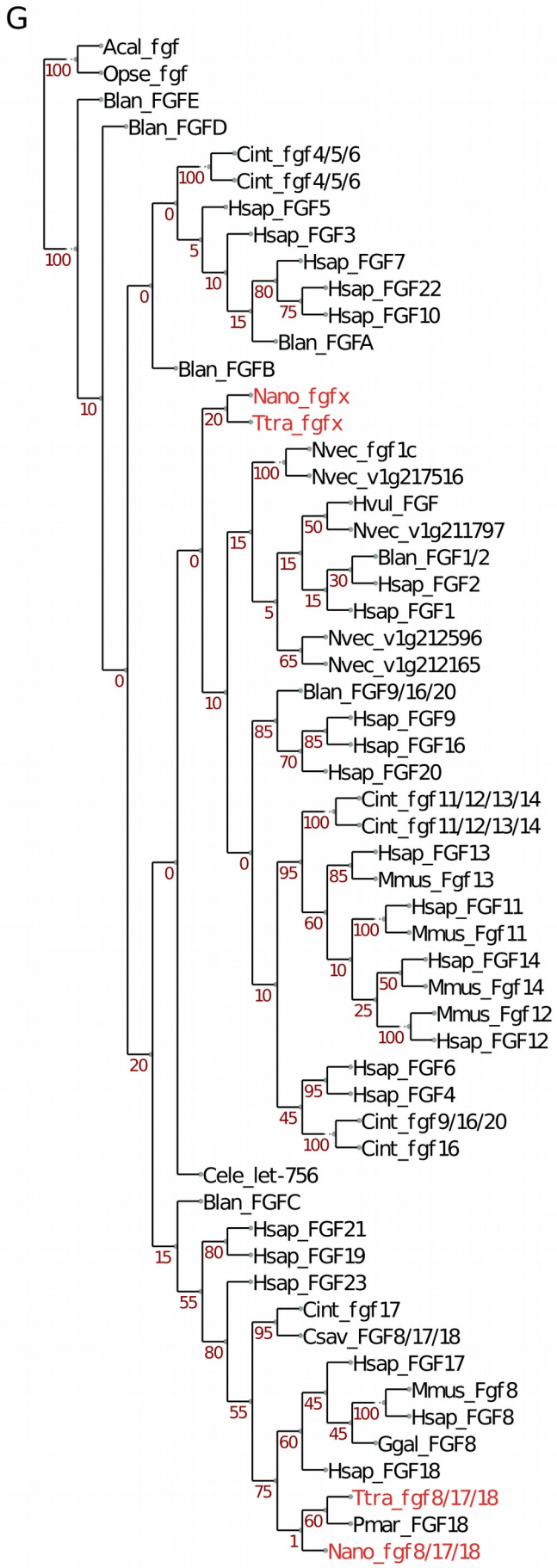

bioRxiv preprint doi: https://doi.org/10.1101/029892; this version posted January 25, 2016. The copyright holder for this preprint (which was not certified by peer review) is the author/funder, who has granted bioRxiv a license to display the preprint in perpetuity. It is made available under aCC-BY 4.0 International license.

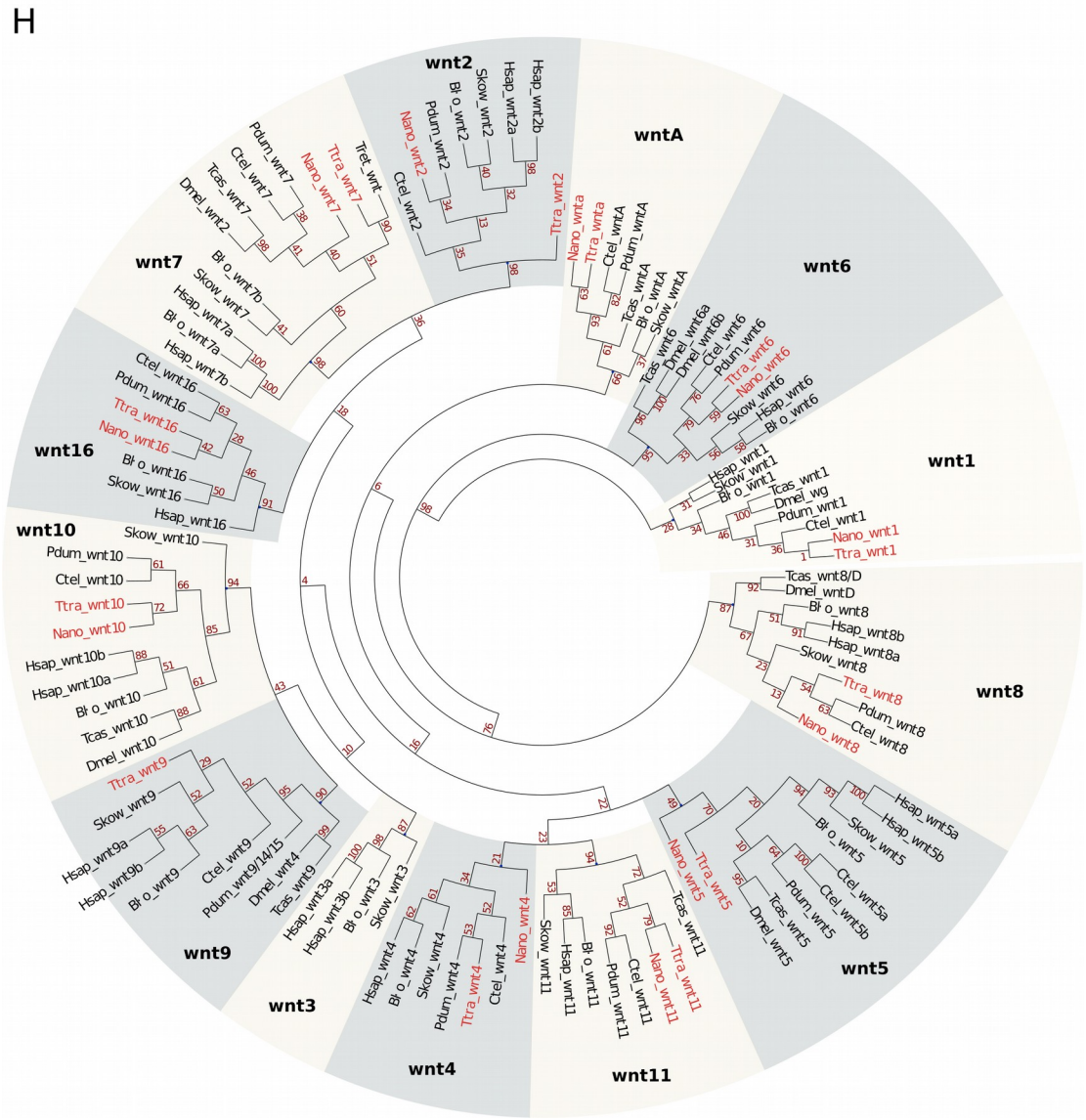

Additional file 6: Figure S4. Orthology assignment for the brachiopod candidate genes used in this study. (A) *hh*. (B) *gli*. (C) *ptc*. (D) *smo*. (E) *en*. (F) *pax*. (G) *fgf*. (H) *wnt*. Cladograms show branch support values and brachiopod orthologs in red.